| Sl. No. | INDIAN INSTITUTE OF TECHNOLOGY ROPAR<br>List of Recent Publications with Abstract<br>Coverage: December, 2024 |
|---|---|
| **A** | **Book Chapter(s)** |
| **1.** | 3D printing for wearable biosensing and energy storage devices<br>**V Vaishampayan, R Kumar**, A Kapoor, **SP Gumfekar** - 3D Printed Smart Sensors and Energy Harvesting Devices: Concepts, fabrication and applications: Book Chapter, 2024<br><br>**Abstract:** This chapter aims to provide an overview of recent advancements in 3D-printed wearable devices with a specific focus on biosensing and energy applications. An overview is given of various additive manufacturing techniques. The materials compatible with different techniques are discussed, and their scope and limitations are identified. Illustrative examples are described for biosensors and energy storage devices in terms of design specifications, manufacturing approaches, and user-oriented applications. A critical evaluation is made of the challenges associated with developing 3D-printed wearable devices. Future directions are identified toward the design and development of multifunctional devices integrated with information technologies for widespread user acceptance. |
| **B** | **Conference Proceeding(s)** |
| **2.** | A 5.4mW 12GHz Quadrature VCO using current reusing technique in 28nm CMOS technology<br>**ZR Sheikh, T Kaur**, R Nagulapalli…**M Sakare** - 2024 15th International Conference on Computing Communication and Networking Technologies (ICCCNT), 2024<br><br>**Abstract:** The quadrature clock (IQ) generation scheme is very important in high-speed SERDES or general 4-way interleaved systems. In this work, a current reusing technique has been exploited, by stacking the VCO, divider, and output buffers. Also, an NMOS/PMOS cross-coupled pair has been used for VCO, which generates a higher 2x swing, unlike the CMOS VCO. A novel digital on/off momcapacitor switch is proposed to minimize its contribution to the VCO phase noise during the 'off' state. The proposal has inherent voltage regulation action resulting in a better PSRR. A prototype has been implemented in 16nm FF technology, which has a 24GHz VCO, and a 12GHz IQ clock divider. The circuit consumes 5.4mW power from a 1.0V supply. The phase noise of the 12GHz carrier frequency at 1MHz offset is -110dBc/Hz while achieving an FOM of -187.5dBc at 1MHz offset. A frequency pushing of 100kHz has been simulated for a 5mV pk-pk 10MHz supply noise. |
| **3.** | A novel charge neutral, programmable, wireless brain stimulation system for rat experiments<br>S Bhaskara, SG KV, S Datta, S Gupta, K Lakshmiramanan, **DM Das**, HJ Pandya - 2024 8th International Conference on Biomedical Engineering and Applications (ICBEA), 2024<br><br>**Abstract:** Deep Brain Stimulation (DBS) of brain regions such as the Subthalamic nucleus (STN) or Globus pallidum internum (GPi) is a clinical therapy for treating the motor symptoms of Parkinson's disease for the last few decades in humans when the drug-induced fluctuations are seen. Still, the regions involved in Parkinson's disease are under constant investigation for better outcomes with respect to gait, and research is actively carried out in this area on various animal models, especially on rats. Stimulator circuits required for electrical excitation of the brain in rat models need to be smaller than the rat's body, lightweight, and tether-free such that behavior is not affected during the experimentation. Parameters such as pulse amplitude and frequency need to be programmable in real-time since the exact values are not known prior. The stimulator needs to maintain charge neutrality such that extra charge should not be injected into the brain, which may adversely affect the experimental outcome. In this work, a wireless biphasic pulse generator |

| | |
|---|---|
| | (weight: 9.89 g without battery, dimensions: 4.3 cm x 3.8 cm) is developed and deployed in an anesthetized rat for intracortical microstimulation of the motor cortex region. A Bluetooth low-energy module integrated with the system facilitates wireless communication. The onboard microcontroller's current DAC unit is programmed to generate sink currents (0-2.04 mA) in real time. The current mirrors used in the design enable simultaneous multi-output pulse generation. The switching logic in the final stage generates biphasic pulses required for brain stimulation that can guarantee charge neutrality as the same network is involved in generating cathodic and anodic pulses. Additionally, the discrete components are chosen so that the turnaround time is less than two weeks compared to ASIC-based approaches, which typically take several months for development and testing. |
| **4.** | Addressing the climate change through CO2 sequestration of GGBFS-added concrete<br>**SK Saikia, K Saini, AS Rajput** - International Conference on Pollution Control for Clean Environment (ICPCCE, 2023), 2024<br><br>**Abstract:** The rising atmospheric $CO_2$ concentration reaching nearly 40 billion tonnes every year has prompted widespread global concern about greenhouse gas (GHG) emissions leading to severe global warming. Carbon-sequestered concrete (CSC) emerges as a promising solution for addressing climate change through utilising $CO_2$ on a significant scale, fostering a sustainable future in the construction industry. Further, integrating green binders such as Ground Granulated Blast Furnace Slag (GGBFS) into conventional concrete could mitigate a substantial portion of approximately 4 billion tonnes of global $CO_2$ emissions annually arising from the calcination processes in cement manufacturing industries. With the aim of harnessing this capacity, the authors attempted to evaluate and enhance the carbon sequestration of GGBFS-added concrete and cement binder types, using a state-of-the-art $CO_2$ mixing and $CO_2$ curing facility. Various investigations were performed to understand its influence on $CO_2$ Uptake Capacity, Strength and Microstructure. This sustainable concrete-producing technology demonstrated a momentous overall $CO_2$ Uptake of 20.04% (which included an enhanced $CO_2$ uptake of more than 13%), thereby showcasing the potential for realising India's ambitious goal of achieving carbon neutrality by 2070. Further, it was able to improve the compressive strength by up to 19.90% and reduce pore sizes to <1 mm on account of densification and microstructure enhancement. |
| **5.** | Attentive color fusion transformer network (ACFTNet) for underwater image enhancement<br>**MU Wani**, MR Khan, **A Kulkarni**, SS Phutke, **SK Vipparthi**, S Murala - International Conference on Pattern Recognition, 2025<br><br>**Abstract:** Underwater imagery often suffers from issues like color distortion, haze, and reduced visibility due to light's interaction with water, posing challenges for applications like autonomous underwater vehicles. To address these obstacles effectively, we introduce the Attentive Color Fusion Transformer Network (ACFTNet) for underwater image enhancement. At the core of our proposal lies a novel Adaptive Dual-Gated Attentive Fusion Block (ADGAFB), which seamlessly integrates localized transmission features and global illumination characteristics. Subsequently, it employs a dual-gated mechanism to generate attentive features for each channel (R, G, and B). To ensure accurate color fidelity, we introduce the Color-Attentive Fusion Block. This block adeptly merges attentive features obtained from each R, G, and B channel, ensuring precise color representation. To selectively transmit features from the encoder to the corresponding decoder, we utilize an Adaptive Kernel-Based Channel Attention Module. Moreover, within the transformer block, we propose a Multi-Receptive Field Feed-Forward Gated Network to further refine the restoration process. Through comprehensive evaluations on benchmark synthetic (UIEB, EUVP) and real-world (UIEB (challenging-60), UCCS, U45) underwater image datasets, our method exhibits superior performance, as verified by extensive ablation studies and comparative analyses. The testing code is available at https://github.com/MohdUbaidwani/ACFTNet. |

| | |
|---|---|
| **6.** | CARDR: DRAM cache assisted ransomware detection and recovery in SSDs<br>**WH Mir, N Goel, VK Tavva** – MEMSYS'24: Proceedings of the International Symposium on Memory Systems, 2024<br><br>**Abstract:** Ransomware has emerged as one of the most prevalent and evolving cybersecurity threat in recent times, posing significant risks due to its potential to cause substantial financial damage and its ability to hold important data hostage. Numerous approaches have been proposed to defend against ransomware at the SSD controller. In this paper, we propose a novel SSD-level defense solution called Cache Assisted Ransomware Detection and Recovery (CARDR), that leverages the DRAM cache of the SSD to counter the potential ransomware attacks. CARDR extracts features from both the DRAM cache and incoming I/O requests for the early detection of ransomware using a machine learning model such as a decision tree. Additionally, CARDR effectively reduces data recovery overhead, making it a robust solution against evolving ransomware threats. Our experimental results demonstrate that CARDR helps in the early detection of ransomware. On average CARDR takes ~ 11 seconds as compared to SSDInsider++ (baseline) which takes ~ 14 seconds for ransomware detection. For data recovery, CARDR reduces the size of the recovery queue by ~ 42% in comparison with the baseline. |
| **7.** | Circuits, proofs and propositional model counting<br>**S Chede**, L Chew, **A Shukla** - 44th IARCS Annual Conference on Foundations of Software Technology and Theoretical Computer Science (FSTTCS), 2024<br><br>**Abstract:** In this paper we present a new proof system framework CLIP (Circuit Linear Induction Proposition) for propositional model counting (#SAT). A CLIP proof firstly involves a Boolean circuit, calculating the cumulative function (or running count) of models counted up to a point, and secondly a propositional proof arguing for the correctness of the circuit. This concept is remarkably simple and CLIP is modular so it allows us to use existing checking formats from propositional logic, especially strong proof systems. CLIP has polynomial-size proofs for XOR-pairs which are known to require exponential-size proofs in MICE [Fichte et al., 2022]. The existence of a strong proof system that can tackle these hard problems was posed as an open problem in Beyersdorff et al. [Olaf Beyersdorff et al., 2023]. In addition, CLIP systems can p-simulate all other existing #SAT proofs systems (KCPS(#SAT) [Florent Capelli, 2019], CPOG [Bryant et al., 2023], MICE). Furthermore, CLIP has a theoretical advantage over the other #SAT proof systems in the sense that CLIP only has lower bounds from its propositional proof system or if $P^{\#P}$ is not contained in P/poly, which is a major open problem in circuit complexity. CLIP uses unrestricted circuits in its proof as compared to restricted structures used by the existing #SAT proof systems. In this way, CLIP avoids hardness or limitations due to circuit restrictions. |
| **8.** | Development of a scanning confocal microscopy to study single quantum emitters<br>**N Singh, RV Nair** - Advances in Nano-Photonics and Quantum Optics (PHOTONICS, 2023), 2024<br><br>**Abstract:** Quantum emitters like the nitrogen-vacancy (NV) centres in diamonds and defects in 2D materials, such as hexagonal Boron Nitride (hBN), represent a promising avenue for stable, room-temperature single photon sources. Such sources have a wide range of potential applications in quantum computing and quantum key distribution. It is required to locate the quantum emitters in the sample to study emitter-specific background-free emission dynamics. We have built a scanning confocal microscopy setup to image single quantum emitters and study their emission dynamics. The study involves emission intensity and decay rate measurements, spin manipulations using an external microwave field, and a single photon source detection using Hanbury Brown and Twiss (HBT) interferometry. The NV centre emission properties are extensively studied using this setup. This technique proves especially valuable for investigating single photon sources, as the accurate localisation of emitters is crucial in such studies. |

| | |
|---|---|
| **9.** | DREAMS: Diverse reactions of engagement and attention mind states dataset<br>**M Singh, G Sharma**…**A Dhall** - International Conference on Pattern Recognition (ICPR, 2024), 2024<br><br>**Abstract:** Active attention and engagement are important in improving users' learning experiences. Engagement refers to the level of involvement and interest individuals show towards a particular task. Attention, on the other hand, refers to a state where someone is entirely focused on a particular task with conscious awareness. Engagement and attention are different but closely linked concepts and can influence each other bidirectionally. To explore the relationship between user engagement and attention, we introduce the *Diverse Reactions of Engagement and Attention Mind States (DREAMS)* dataset. The dataset includes facial video recordings of 32 users in naturalistic settings watching various stimuli to evoke diverse emotions. We then analyze user engagement and attention states in these videos by framing it as a classification problem, exploring single-task, transfer learning task, and multi-task settings. In single and transfer learning task settings, separate networks are applied to predict engagement and attention states. Whereas in multi-task settings a shared network is applied, which jointly learns to predict both engagement and attention states. Moreover, we examine participants' performance on video-based questionnaires and evaluate their perceived cognitive workload. In our findings, we observe (a) better classification performance in predicting engagement states in both transfer and multi-task learning compared to single-task learning and (b) higher engagement and attention states correlate with lower cognitive load and improved task performance. The dataset and the code are publicly available and can be accessed through https://sites.google.com/view/dreams-dataset/dataset. |
| **10.** | Enhancing resilience of WPT systems to lateral misalignment using near-field coil antennas<br>**A Bharadwaj, CC Reddy, A Sharma** - 2024 IEEE 5th India Council International Subsections Conference: Science, Technology and Society, 2024<br><br>**Abstract:** The article presents an experimental validation of the author's hypothesis stating the Tx coil antenna, capable of forming a widespread uniform magnetic field, attains constant output current (C-O-C) and constant output voltage (C-O-V). Aiming this, a previously published NUDCT Tx coil antenna was adopted to form a uniform magnetic field. Additionally, with the aid of in-house high-frequency inverters and rectifier circuits, the authors experimentally attempted to prove C-O-C and C-O-V. As a result, this eliminates complex control circuits, higher-order compensation networks, and additional dc-dc converters at the Rx side. Moreover, the Tx coil antenna is fabricated using three different materials to validate the enhancement of dc-dc efficiency by employing low-loss materials without altering the optimized parameters of the Tx coil antenna. |
| **11.** | Experimental investigation of photocatalytic efficiency of TiO2 in reducing urban air pollution<br>**S Mishra, P Zende, P Haldar, I Dadha** - International Conference on Pollution Control for Clean Environment (ICPCCE, 2023), 2024<br><br>**Abstract:** Photo-catalysis is widely used for the treatment of air pollution caused by the emission of pollutants and harmful gases like volatile organic compounds (VOCs) from indoor and outdoor sources. Some VOCs are carcinogenic and degrades very slowly in the atmosphere. A major part of our time we spent indoors inside some infrastructure whether it is a residence or workplace, where we are exposed to those pollutants frequently. This paper investigates the photocatalytic efficiency of $TiO_2$ in reducing such air pollutants when applied over the building surface. To accomplish the goal, cement mortar samples are prepared with various doses of $TiO_2$ (ranging from 6.18E−03 to 41.2E−03 g/cm$^2$) and investigated further for the rate of degradation of VOCs inside batch reactors in the presence and absence of sunlight. The obtained results showed the variation of degradation rate from 0.9E−04 to 1.7E−4 min$^{-1}$ cm$^{-2}$ for various initial concentrations of TVOC in the range of 600–2900 ppm over 600 min. The selected |

| | |
|---|---|
| | approach demonstrated the maximum degradation rate constant of 5.4E−04 $min^{-1}$ $cm^{-2}$ corresponding to 15% of $TiO_2$ dose by cement weight. This shows the viability of $TiO_2$ in the purification of polluted air and advocates its widespread use on building surfaces. |
| **12.** | Explaining the identification of granular crack with deep learning and xai<br>**A Pratap, N Sardana** - 2024 IEEE Region 10 Symposium (TENSYMP), 2024<br><br>**Abstract:** Precise detection of granular fractures is crucial for various engineering applications, and Deep Learning approaches can transform imaging methodologies and material analysis. This study employed a convolutional neural network (CNN) that incorporated explainability elements to improve the trustworthiness and transparency of the model in classifying granular cracks. After conducting thorough model comparisons and analyses, a bespoke model was chosen. Extensive model comparisons and analyses led to the selection of a custom model with 91% training accuracy and optimized parameters. Fine-tuning of six pre-trained models identified VGG-16 as the top performer, achieving 99.96% training accuracy and 97.7% testing accuracy. Explainable AI (XAI) techniques, particularly the insertion method, provided robust interpretability, with attributed scores of 0.96 for insertion, 0.69 for deletion, and 0.37 for fidelity. Visualization using various attribution mapping methods reinforced the trustworthiness of this work in granular crack identification. |
| **13.** | Frequency modulated deformable transformer for underwater image enhancement<br>A Dukre…**A Kulkarni**…**SK Vipparthi**…S Murala - International Conference on Pattern Recognition, 2025<br><br>**Abstract:** Underwater images frequently experience quality degradation due to refraction, back-scattering, and absorption, leading to color distortion, blurriness, and reduced visibility. Such degradation present in the underwater images can cause inaccuracies while functioning with higher advanced level computer vision applications, equipped for autonomous underwater vehicles. Despite the ability of enhancing the degraded images, existing approaches fail at preserving the localized fine edges also producing the true colors. Therefore, an effective pre-processing network is necessary for underwater image enhancement. With this motivation, we propose a frequency modulated deformable transformer network for underwater image enhancement. Initially, the features are extracted with the proposed multi-scale feature fusion feed-forward module. Further, the frequency modulated deformable attention module is proposed to reconstruct fine-level texture in the restored image. Here, we propose a spatio-channel attentive offset extractor in the modulated deformable convolution for focusing on relevant contextual information. Also, adaptive edge-preserving skip connections are proposed for propagating prominent edge features from the network's shallow layers to its deeper layers. A comprehensive evaluation of the proposed method on synthetic and real-world datasets and extensive ablation analysis demonstrates that the proposed approach shows superior performance than existing state-of-the-art methods. The testing code is provided at https://github.com/adinathdukre/FMDTUIE. |
| **14.** | Fusing image and text features for scene sentiment analysis using whale-honey badger optimization algorithm (WHBOA)<br>PS Yadav, DK Tyagi, **SK Vipparthi** - International Conference on Pattern Recognition, 2024<br><br>**Abstract:** Developing a real-time sentiment analysis application that relies solely on features extracted from images or textual content falls short of capturing human emotions' nuanced and multifaceted nature. The unlabeled dataset, though useful, has limitations for sentiment analysis due to its general image descriptions, which lack emotional depth and do not include direct sentiment labels. Finding scene sentiment is a challenging task. To address this, combining textual descriptions with visual features is crucial. Important parameters include entropy, bag of |

| | |
|---|---|
| | words, and parts of speech (nouns, adjectives, and verbs) for textual analysis, alongside visual features like SIFT, SURF, and color histograms. These features are integrated to capture a comprehensive range of sentiment cues, enhancing the accuracy and depth of sentiment insights. This paper proposes an optimized adaptive neuro-fuzzy inference system for a compelling feature enhancement using the Whale-Honey Badger Optimization Algorithm (WHBOA). The proposed method identifies the most relevant and effective features from both textual and visual data. It captures visual-specific attributes to provide a richer and more detailed representation of visual content, addressing the limitations of general image descriptions and paving the way for the development of predictive models. Additionally, text pre-processing cleans and normalizes the textual data. We conducted an extensive comparative performance evaluation to assess the effectiveness and accuracy of the proposed model. The model is compared with the Nearest Neighbor, Support Vector Machine (SVM), and Decision Tree classification algorithms for the performance assessments.The results demonstrate that the optimized model performs better, achieving an accuracy of approximately 91.2%, compared to the other models. |
| **15.** | Numerical analysis of miniature disk bend specimens under creep condition<br>R Gupta, **AK Mishra**…**A Tiwari** - Structural Integrity Conference and Exhibition (SICE, 2022), 2024<br><br>**Abstract:** Since it only requires a small surveillance sample, small punch creep test (SPCT) analysis has been used to estimate the lifespan of power stations and nuclear reactors. As the specifications in uniaxial creep test (UCT) and SPCT differ, numerous correlations have been proposed for calculation of conventional tensile characteristics for elastic plastic behavior of metallic materials. Due to the high operating temperatures in nuclear power plants and highly developed ultra-super critical plants, many of the components experience creep deformation. In order to determine how long a component will last, it is crucial to understand the correlations between creep properties calculated through SPCT. Thin disk specimens subjected to SPCT can be thought of as a helpful method for identifying the creep characteristics of components exposed to high temperatures. The challenge is to estimate the conventional bulk creep properties from a small punch sample. Finite element analysis (FEA) of SPCT of a metallic material can help in estimation of bulk properties and therefore FEA of a metallic material having $E/Y_S$=277 with a power law creep behavior is carried out using ABAQUS software. This particular paper focuses on the influence of specimen thickness on the site of maximum stress, sometimes known as the weakest section, when the punch travel time was varied. |
| **16.** | PiExtract: An end-to-end data extraction pipeline for pie-charts<br>**MS Kanroo, HS Kawoosa, J Dhar, P Goyal** - International Conference on Pattern Recognition, 2025<br><br>**Abstract:** Charts are important non-textual elements present in documents, providing a visual representation of numerical data. Among different representations, Pie-charts are commonly employed in digital documents due to their perceptual advantages for displaying numerical data and inter-relationship information. Chart Data Extraction is a multi-stage pipeline, with each stage playing a crucial role in obtaining the raw data correctly. Prior work mostly focuses on improving the performance of one or a combination of a few sub-stages. In this work, we propose a novel end-to-end data extraction algorithm, PieExtract, to extract data from pie-charts. This proposed algorithm designs a novel Robust Fusion Attention Network (RobFA-Net) approach for chart classification tasks. This network introduces a robust fusion attention strategy to learn significant discriminative global and local information, thereby enhancing the learning model performance. In addition, our novel rule-based sector data extraction method further enhances its performance in extracting data from pie-charts. Extensive experimentation is conducted on three datasets, specifically Revision, Chagas, and FigureQA, focusing on chart classification and the FigureQA dataset for data extraction from pie-charts. Our findings |

| | |
|---|---|
| | demonstrate that the proposed pipeline outperforms compared to previous works, showcasing superior performance. |
| **17.** | Probing attention-driven normalizing flow network for low-light image enhancement<br>**S Singh**…**SK Vipparthi**, S Murala - International Conference on Pattern Recognition, 2025<br><br>**Abstract:** Existing low-light image enhancement approaches based upon pixel-wise reconstruction losses are inadept at capturing the complex distribution of well-exposed images, resulting in residual noise, insufficient illuminance, and artifacts. Additionally, the mapping relationship between weakly-illuminated and normally exposed images is one-to-many, making low-light image enhancement a vastly ill-posed problem. In this work, we probe into this one-to-many relationship via an attention and frequency driven normalizing flow network by minimizing the negative log-likelihood loss. The proposed model comprises of two parts: a dual-attention-oriented frequency encoder network and an invertible network which inputs the conditional low-light images and changes the mapping of the complex distribution of well-light images to simpler Gaussian distribution. The proposed model not only utilizes the spatial information inherent in the image for improving the contrast but also extracts the frequency information for preserving the intricate details. To sum up, the distribution of the well-exposed images can be characterized better, and the overall enhancement mechanism becomes analogous to being restrained by a loss function which defines the manifold structure of natural images during the training. Detailed experiment analysis on a variety of challenging low-light images exemplifies the potency of the model and shows its primacy over the state-of-the-art in terms of enhanced quality and efficiency. |
| **18.** | PROLONG: Priority based write bypassing technique for longer lifetime in STT-RAM based LLC<br>**P Sinha**, KP BV, S Das, **VK Tavva** - Proceedings of the International Symposium on Memory Systems, 2024<br><br>**Abstract:** The rise of data-driven applications requires larger on-chip Last Level Caches (LLCs) in multicore systems which need denser chips with lower power consumption. Non-Volatile Memory (NVM) technologies such as Spin-Transfer Torque RAM (STT-RAM) based LLCs fulfill these requirements. STT-RAM based LLCs suffer from notable shortcomings, including higher write latency, increased write power consumption, and limited endurance. The primary cause of the low write endurance of an STT-RAM based LLC is the uneven distribution of write operations across the cache. To address the challenge of low write endurance in an STT-RAM based LLC while minimizing performance impact, we propose a unique inter-set wear leveling technique. It involves aggressively bypassing the write-back requests coming to the LLC from upper level of cache memories and writing directly to the main memory. Only those bypassed writes, which may be accessed again in the future, are stored in an SRAM buffer. Bypassing writes for a specific block in the LLC to SRAM Buffer or Main Memory is contingent upon satisfying certain conditions based on the set-wise write count and the priority of the block. Through extensive computational analysis, we have determined that the application of this technique in a quadcore setup reduces inter-set write variation by 84% and intra-set write variation by 19%. A lifetime improvement of 35 times as compared to the baseline STT-RAM based LLC can be achieved. Importantly, our approach maintains the system performance. |
| **19.** | Some experiments on thermal aging of XLPE underground cables<br>**HK Azmeera, CC Reddy** - 2024 10th International Conference on Condition Monitoring and Diagnosis (CMD), 2024<br><br>**Abstract:** Thermal stress effects on the insulation material of high voltage underground cables plays a significant role in assessing the working life. Experimental based thermal aging tests are performed on a widely used high voltage cable insulation in this study. The cable in its entirety is |

| | |
|---|---|
| | aged at three different temperatures for a duration of 12 months. The subsequent changes in the electrical and morphological properties are studied. Dielectric breakdown test along with dielectric constant and dielectric loss tan (δ) analysis is done to determine the electrical property changes. FTIR and XRD are done to understand the morphological changes. The results obtained provide the temperature at which the material degradation is least and performance is not hindered. |
| **20.** | U-ENHANCE: Underwater image enhancement using wavelet triple self-attention<br>**P Mishra, SK Vipparthi**, S Murala - Proceedings of the Asian Conference on Computer Vision, 2024<br><br>**Abstract:** Transformer-based methods have demonstrated remarkable performance in underwater image enhancement due to their ability to capture long-range dependencies, crucial for high-quality reconstruction of degraded images. However, existing Transformer-based techniques often treat all token similarities equally during self-attention, which can lead to the aggregation of irrelevant features, hampering clear image restoration.We propose U-ENHANCE, a novel Underwater image Enhancement framework that integrates wavelet-based frequency decomposition with spatial domain attention to address these challenges. In particular, we introduce a Wavelet Triple Self-Attention (WTSA) mechanism that performs self-attention across three dimensions--horizontal, vertical, and channel-wise, effectively capturing multi-scale features critical for restoring fine details and structural integrity. Additionally, we design a Self-Calibrated Feedforward Network (SCFN) that refines feature representation by dynamically adjusting the receptive field, further enhancing spatial and frequency domain integration. Extensive experiments on underwater image enhancement benchmarks demonstrate that U-ENHANCE outperforms state-of-the-art methods by providing superior restoration of color, clarity, and structural details. The code is available at: https://github.com/Priyanka01mishra/UENHANCE. |
| **21.** | Uncertainty-RIFA-Net: Uncertainty aware robust information fusion attention network for brain tumors classification in MRI images<br>**J Dhar, K Rana, P Goyal** - International Conference on Pattern Recognition, 2024<br><br>**Abstract:** Malignant brain tumors pose a significant global threat, emphasizing the critical need for efficient diagnostic methods utilizing MRI. Manual analysis of MRI images is labor-intensive and subjective, highlighting the necessity for faster and automated effective methods. In this paper, we propose an uncertainty-aware robust information fusion attention network model for precisely classifying brain tumors in MRI images. Our approach introduces a novel robust information fusion attention layer that learns enhanced representations by integrating global context with local information. We estimate the uncertainty in our model's predictions using the ensemble Monte Carlo dropout strategy. Our findings demonstrate outstanding performance, achieving accuracies of 98.37% on the Cheng dataset and 98.48% on the Nickparvar dataset in brain tumor MRI image classification tasks, while minimizing computational costs in terms of resource usage and inference time. |
| **22.** | WARMOS: Enhancing weather-affected referred moving object segmentation<br>P Saxena…**SK Vipparthi**, S Murala - Proceedings of the Asian Conference on Computer Vision, 2024<br><br>**Abstract:** Environmental noise, such as haze and rain, poses significant challenges in video surveillance, in tasks like referred video object segmentation. These weather-related disturbances introduce excessive pixel variance, making moving object segmentation more complex. In this work, we focus on addressing the issue of adverse weather conditions by simulating the effects of haze and rain in videos and employing a robust noise removal model. The model effectively reduces pixel variance caused by environmental factors. This enhanced framework is precious |

| | |
|---|---|
| | for referred moving object segmentation, where objects identification done based on text queries. By integrating our noise removal module, we ensure better alignment of features, which enhances the precision of referred moving segmentation. Our approach maintains temporal consistency, making object segmentation more reliable under challenging weather conditions while preserving the original video quality by removing weather noise. We have employed separate noise removal modules for haze and rain environmental noise. A ResNet based classifier model trained to identify the noise class on the fly. To demonstrate the effectiveness of our methodology, we selected an ROV benchmark to assess segmentation performance. Experiments on the DAVIS 2017 dataset show that our proposed methodology performs well on weatheraffected videos, significantly improving the benchmark metrics Jaccard (J) and F-measure (F) indices after removing weather noise. Using the benchmark SgMg model for referred segmentation, the mean J&F score is 63.64 without environmental noise. When haze is introduced to the dataset, the mean J&F score drops to 58.71. After applying WARMOS approach, the mean J&F improves to 60.50. A similar pattern is observed for rain: when rain is introduced, the mean J&F score is 61.00, and after applying WARMOS, it improves to 61.06. This highlights our approach's significance in mitigating the impact of environmental noise. |
| **C** | **Journal Article(s)** |
| **23.** | 6,6′-Biindeno[1,2-b]fluorene: an open-shell indenofluorene dimer<br>**H Sharma**, P Jana, D Mallick, S Bandyopadhyay, **S Das** - Chemical Science, 2024<br><br>**Abstract:** Nakano *et al.* reported that the antiaromatic indenofluorene (IF) isomers are diradicaloid molecules having varying degrees of open-shell character, with indeno[1,2-*b*]fluorene displaying a weaker diradical character index ($y_0$ = 0.072). Unlike 6,12-trimethylsilylethynyl disubstituted [1,2 -*b*]IF, the 6,12-aryl disubstituted [1,2-*b*]IF derivatives did not show any experimental evidence of diradical properties. This raised the question of whether a [1,2-*b*]IF dimer would prefer a closed-shell or an open-shell ground state. To address this, herein we report the synthesis of a 6,6′-biindeno[1,2-*b*]fluorene derivative, which is a [1,2-*b*]IF dimer, constructed by linking two [1,2-*b*]IF units with a C–C single bond at carbons 6 and 6′ bearing the largest orbital coefficients for the highest occupied and lowest unoccupied molecular orbitals (HOMO and LUMO). The C6–C6′ linkage effectively narrowed the HOMO–LUMO gap while the strong desire to avoid *s*-indacene antiaromaticity restored two Clar sextets in two proaromatic *para*-quinodimethane subunits, resulting in an open-shell bifluorenylidene-type diradicaloid ($y_0$ = 0.268) ground state with minor tetraradical character index ($y_1$ = 0.007). The open-shell nature was confirmed by single crystal X-ray and electron paramagnetic resonance analyses, and supported by theoretical calculations. |
| **24.** | A comprehensive review on carbon-based thermal sprayed coatings for orthopedic implants<br>**S Singh, H Singh, K Rakha** - Journal of Thermal Spray and Engineering, 2024<br><br>**Abstract:** The use of orthopedic implants is increasing worldwide as the population of older people is growing. Metals and their alloys like stainless steel, cobalt-chromium alloys, and titanium alloys are widely used as implant biomaterials for the treatment of orthopedic joint failure because of their biocompatibility and good mechanical properties. However, these materials offer poor osseointegration due to their bio-inert nature. Hydroxyapatite, a bioactive material, has similar properties to bone tissue and helps in improving bone regeneration. It has good osseointegration properties, but it lacks mechanical properties. It has low fracture toughness, wear resistance and poor tensile strength. The carbon reinforced hydroxyapatite can have better mechanical properties as well as biocompatibility. The addition of graphene and carbon nanotubes in HA can also provide antibacterial effects and induce osteogenic differentiation of stem cells. The surface modification process like surface coatings involves the addition of composite materials to have desirable properties. The hydroxyapatite coatings produced by thermal spray are commercially accepted by FDA (Food and Drug Administration). |

| | |
|---|---|
| | Thermal spray materials can play a vital role in enhancing orthopedic implants' biocompatibility, wear, and corrosion resistance. The coatings can improve the optimal integration to the surrounding tissues and result in increasing the life of implants. The study will focus on the various thermal spray techniques like flame spray, HVOF (High-Velocity Oxygen Fuel), cold spray, and plasma spray that are commonly used in bio-implant applications. The paper will also discuss the different types of biomaterial coatings produced with thermal spray processes by the researchers. Moreover, the comparison of various thermal spray coatings for biomedical applications are also covered. |
| **25.** | A coupled thermo-mechanical model for warm single-point incremental forming process<br>**N Kumar, M Mahala, A Agrawal** - Archives of Civil and Mechanical Engineering, 2024<br><br>**Abstract:** Single point incremental forming (SPIF) is a low-cost, low-volume forming technique that has gained the attention of researchers over the past two decades. However, it has primarily been utilized for ductile materials such as aluminum and steel alloys and has yet to be extensively explored for hard-to-form materials such as magnesium (Mg) alloys, which are widely used in aviation and automotive industries. The hexagonal close-packed structure of these alloys makes it challenging to deform at room temperature. Studies have shown that the formability of Mg alloys can be increased under warm forming conditions. The analytical model needs to be developed to understand the effect of temperature on material properties and process parameters and their dependencies on each other. The present work proposes an analytical thermal model to predict in-plane strains during the warm SPIF process of magnesium (AZ31B) alloy. A coupled thermo-mechanical numerical simulation model was developed using ABAQUS/EXPLICIT® software to estimate in-plane strains and thickness distribution. The Johnson–Cook model was applied to define the fracture criterion and the constitutive model. The predictions of the analytical and numerical models developed in this study were compared with experimental results. Further, the study investigated the impact of step depth, tool diameter, and wall angle on formability and thickness distribution. The predictions from the model developed in this study take significantly less computational time than numerical simulation analysis with an accuracy within 3% of the numerical model. |
| 26. | A custom deep learning model for abiotic stress classification in maize in uncontrolled environments<br>P Goyal, R Sharda, S Thaman, **M Saini** - Computers and Electronics in Agriculture, 2025<br><br>**Abstract:** Global food production, especially cereal crops such as maize, is seriously affected by abiotic plant stresses, which negatively impact yields and concern global food security. Modern imaging methods like deep learning have revolutionized plant stress estimation. In this study, we propose a novel convolutional neural network (CNN) architecture tailored to discern and categorize different types of abiotic stress in maize under diverse environmental conditions. A custom dataset of 6035 RGB images was acquired during the open field trials conducted at the research farm of Punjab Agricultural University, Ludhiana, in the year 2021–22 to classify nutrient stress of nitrogen, phosphorus, and potassium as well as water-deficit stress from the healthy images of maize crops. The custom CNN model was structured around four distinct feature blocks consisting of different combinations of convolution, batch normalization, pooling, and dropout layers as iterations. The dataset was partitioned into training, validation, and test sets in a ratio of 7:2:1. Iteration B, which comprised only dropout as a regularization layer, performed the best compared with the other iterations. Iteration B achieved accuracies of 95.64, 98.09, and 97.04% for the training, validation, and test sets, respectively. The developed CNN models can be further integrated with decision support systems, such as mobile applications, for real–time plant stress assessment in maize crop by farmers at the field level as an alternative to physical plant color guides. |

| | |
|---|---|
| **27.** | A novel approach for image retrieval in remote sensing using vision-language-based image caption generation<br>PS Yadav, DK Tyagi, **SK Vipparthi** - Multimedia Tools and Applications, 2024<br><br>**Abstract:** Recent advancements in satellite technologies have resulted in the emergence of Remote Sensing (RS) images. Hence, the primary imperative research domain is designing a precise retrieval model for retrieving the most pertinent images based on the query. Present Remote Sensing Image Retrieval (RSIR) systems use visual descriptors to characterize the primitives (such as various land-cover types) that are visible in the images. However, the visual descriptors are inadequate for defining the complicated content of RS images. To solve this problem, a new model is devised for image retrieval based on image captions. The goal is to generate textual illustrations with captions to define relations amongst objects precisely. Here, image captioning is attained based on the vision-language pre-training model. The image captions are utilized for generating features like term frequency-inverse document frequency (TF-IDF), length of text, and Bag of Words. Meanwhile, query text is utilized wherein features like TF-IDF, text length, and Bag of Words are obtained. The similarity between query text features and the image captions features has been computed on the basis of a hybrid similarity measure wherein weights are tuned with the proposed Honey Badger Political Optimizer (HBPO) to retrieve the image. The proposed HBPO provided enhanced efficiency with elevated precision of 93.3%, recall of 93.7%, F1-score of 93.5%, and Recall-Oriented Understudy for Gisting Evaluation (ROUGE) of 0.441. |
| **28.** | A review on framework (MOF/COF/POP)-based materials for efficient conversion of $CO_2$ to bio-active oxazolidinones<br>**P Rani**, R Das, **CM Nagaraja** - Inorganic Chemistry Frontiers, 2025<br><br>**Abstract:** Excessive reliance on fossil fuels has increased atmospheric $CO_2$ emissions, resulting in the greenhouse effect that endangers global climate stability and human well-being. Consequently, the storage and chemical conversion of $CO_2$ into sustainable products can play a vital role in reducing anthropogenic emissions. Hence, there is an upsurge in research on selective carbon capture, sequestration and utilization (CCSU) to mitigate the rising atmospheric $CO_2$ concentration. Carbon capture and utilization (CCU), in particular, has attracted considerable interest because it enables the utilization of $CO_2$ as a C1 feedstock for generating commodity chemicals and fuels such as cyclic or polycarbonates, cyclic carbamates, oxazolidinones, formamides, methane, methanol and so on. Among these products, oxazolidinones are essential five-membered heterocyclic compounds found in several important pharmaceuticals. Oxazolidinones also function as versatile intermediates and chiral agents in organic synthesis. Thus, developing highly efficient heterogeneous catalysts containing dense basic and catalytic sites is potentially significant for effectively capturing and transforming $CO_2$ into 2-oxazolidinones under ambient conditions. In this regard, porous framework-based materials *viz* metal–organic frameworks (MOFs), covalent organic frameworks (COFs) and porous organic polymers (POPs) are excellent candidates owing to their fascinating attributes, like ample active sites, intrinsic porosity and accessible functionalities. These framework-based materials have been exploited as recyclable catalysts in efficient cyclization of $CO_2$ with aziridines, propargylic amines and alcohols coupled with amines/epoxides to produce oxazolidinones. This review provides a detailed analysis of recent advancements in developing porous framework-based recyclable catalysts for environmentally friendly conversion of $CO_2$ to oxazolidinones. Furthermore, future considerations and challenges for fabricating efficient framework-based catalysts in transforming $CO_2$ into value-added oxazolidinones are also discussed. |
| **29.** | Abrupt autofocusing of circular Airy derivative beams in complex media<br>**A Kumari, V Dev, V Pal** - Optics & Laser Technology, 2025 |

| | |
|---|---|
| | **Abstract:** Controlling light propagation through complex media plays a significant role in a wide range of applications ranging from astronomical observations to microscopy. Although, several advances have been made based on adaptive optics, optical phase conjugation and wavefront shaping, but many of these involve challenges such as complexity in design and slow response time. Recently, controlling light propagation in complex media by simply structuring light has shown promising capabilities, and has attracted considerable interests. We present experimental and numerical investigations of abrupt autofocusing of circular Airy derivative beams (CADBs) in complex media. We find that up to a relatively high strength of turbulence, the CADB possesses relatively good abrupt autofocusing, however, the efficiency and autofocusing position (longitudinal and transverse) vary with the strength of turbulence. Further, the spatial distortions in CADB caused by turbulence are quantified by an overlap integral, which shows that CADB possesses reasonably good resilience against the turbulence. The diffraction efficiency (η) of CADB changes by a factor of ∼1.7 with increasing strength of turbulence from zero to high, indicating good confinement of intensity at autofocusing. The focused beam spot size grows gradually with increasing the strength of turbulence, specifically, it grows by a factor of ∼2 for a strong turbulence, indicating reasonably good focusing abilities. The results of CADB are compared with a Gaussian beam, and find that CADB possesses superior focusing abilities in turbulent media. We have carried out a detailed analysis of these observations based on Zernike polynomials, which reveals that different kinds of aberrations present in turbulent media leads to distortions in the spatial structure as well as other properties of CADBs. The simulation and experiment results show good agreement, and the results can be used for various applications, such as in biomedical treatment, seismology, optical tweezers and material processing. |
| **30.** | Accelerators and hurdles, and their mediating effects on electric vehicle adoption<br>**H Ahmad, TM Rahul**, NK Asija - Transport Policy, 2025<br><br>**Abstract:** The sale of electric vehicles (EVs) in India was only 1.32% of all vehicle sales for FY 21–22. Through this study, the authors sought to contribute to the nascent field of research regarding the constructs influencing this low adoption. The study explores the existence of 'early adopters' among Indian consumers and investigates the direct and indirect impact of environmentalism on EV purchase propensity. The causal factors of the variation in the market shares of electric two-wheelers and electric cars in India's EV sales are addressed by estimating two Structural Equation Models encompassing latent variables and socio-demographics influencing their uptake. *Technological Affinity* emerged as the prime motivator and Concerns about Charging and Battery as the key hindrance to electric car purchase propensity. Environmental Consciousness positively affects both electric two-wheelers and electric car purchase propensities indirectly through *Awareness about EVs & Green Policies*, which itself demonstrates a positive influence in both cases. The results suggest that in India marketing electric cars as technologically superior cars rather than eco-friendly cars would be more effective. Concerns about Charging and Battery remained insignificant in the case of electric two-wheelers, lending an explanation to their greater market share despite inadequate infrastructure. |
| **31.** | Advances in understanding silk materials and its nano-photonic applications<br>B Panda, **R Ahuja**, KP Singh - Nano Energy, 2024<br><br>**Abstract:** Silks derived from spiders and silkworm cocoons represent a unique class of protein-based multifunctional materials characterized by exceptional mechanical, biological, and structural properties. Here, we review recent progress in understanding the silk material system, highlight its hierarchical molecular structure and discuss an atomistic model of silk and its success in explaining unique mechanical and optoelectronic properties. We summarize the extraordinary tensile and unique torsional properties of silks and their remarkable resilience under extreme conditions, such as cryogenic temperatures and high vacuum. A notable |

| | |
|---|---|
| | advancement is in nano-processing and heterostructuring of silk fibres using intense femtosecond pulses. This technique facilitated the development of a new class of nano-scale force and torque silk-based sensors operating in air or vacuum and offering high sensitivity. Additionally, cocoon silk, specifically the protein fibroin, is highlighted as a bulk material with significant potential for the fabrication of optical components and both active and passive optoelectronic devices for biomedical applications. Finally, we point out key challenges in this field, such as achieving a complete atomistic understanding of silk materials and discuss emerging opportunities for silk-based functional technological applications.<br> 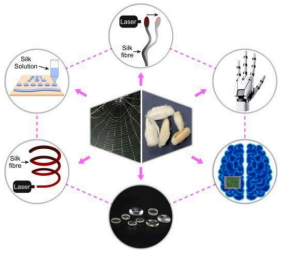 |
| **32.** | Advancing multi-weather resilient roof: Experiment augmented multifaceted thermal parameter analysis with integrated hexad PCMs under tropical steppe climate<br>**AB Huluka, S Muthulingam** - Building and Environment, 2025<br><br>**Abstract:** Effective thermal energy management of building envelopes, particularly roofs, is critical for reducing space cooling demands in tropical steppe climate. Phase Change Materials (PCMs) are being extensively studied for this purpose. Still, most research focuses on single PCM integration, constrained by specific melting points and efficiency under limited weather conditions. This study develops and experimentally investigates a multi-weather roof by integrating hexad PCMs into a two-way hollow concrete roof (TWHCR). The core of the TWHCR is divided into six PCM-integrated strips, grouped into two sets: S-OM30, S-OM35, S-OM42 on one side and S-OM32, S-OM37, S-OM46 on the other, creating a thermal buffering effect, while outer region functions as a conventional concrete strip (S-RCC). The outdoor thermal performance of roof is assessed by analyzing temperature profiles, thermal damping, performance index, load levelling, heat flux variations, and overall heat gain. During testing, each PCM strip's activity varied with ambient temperatures, activating or deactivating as needed to enhance overall thermal performance. S-OM30 showed the most significant temperature reduction increase between February and March (+35.4 %) before dropping in April (−34.3 %), while S-OM42 steadily rose through May (+26.0 %). All PCM strips were rated Good in March, but all were rated Fair by April due to increased thermal stress. In July, S-OM37 and S-OM35 maintained high thermal damping. S-RCC consistently exhibited higher heat flux, with other strips outperforming it by 50 % to 70 %, peaking at 65 % in August. S-OM35 showed the highest efficiency increase from February to March and remained the most efficient in July. |
| **33.** | An approach to regional flood frequency analysis for general peak discharge distribution datasets<br>**AK Singh, SR Chavan** - Journal of Hydrology, 2024<br><br>**Abstract:** Design flood estimation corresponding to various return periods for ungauged or partially gauged sites plays a crucial role in the design of hydraulic structures. Conventional index flood (CIF) approach in the L-moment framework has widely been used which assumes that in a given homogeneous region, all at-site data that is normalized by a central indicator (such as mean or median) exhibit an identical distribution. The present study proposes an approach to perform regional flood frequency analysis (RFFA) for the general peak discharge distribution datasets, wherein the at-site peak flood data is normalized with the central indicator and then transformed into normal distribution using Box-Cox transformation strategy. The proposed approach has been formulated in both L- as well as LH-moment framework. The efficacy of the approach is demonstrated using the Monte Carlo simulation experiment for different length of datasets. Subsequently, the approach is validated using leave-one-out cross validation (LOOCV) |

| | |
|---|---|
| | procedure. The validation of the new approach in the real-world scenario is performed using the annual maximum peak series data of 1173 sites in the conterminous United States and 115 sites in south Indian catchment of Indian region for different return periods. The grouping of sites is performed using region of influence (ROI) approach. The outcomes of the performance measures from the simulation experiments and real-world scenario indicates that the proposed transformation-based approach provides either comparable or better estimates of design floods than CIF approach, especially in the case of mis-specification of regional distribution. |
| **34.** | An opportunity for streamlined computational fluid dynamics integration via a semi-analytical method for weighted finite volume fragmentation equations<br>**S Yadav, D Wadhwa**, M Singh, **J Kumar** - Physics of Fluids, 2024<br><br>**Abstract:** Over the past decade, finite volume schemes have significantly advanced, becoming well-regarded for solving linear and nonlinear population balance equations (PBEs). These schemes are highly accurate and efficient, making them ideal for applications like liquid–liquid dispersion, bubble and droplet fragmentation, in the chemical and pharmaceutical industries. Solving PBEs in continuous form remains challenging, particularly with complex fragmentation kernels and selection functions. Typically, these problems are tackled by forming discretized ordinary differential equations, with accuracy depending on the mesh type and cell count. To address these challenges, a new semi-analytical approach for solving the weighted finite volume scheme breakage equations has been developed [Kumar *et al.* (2015), "Development and convergence analysis of a finite volume scheme for solving breakage equation," SIAM J. Numer. Anal. 53(4), 1672–1689]. This approach can replace traditional numerical schemes using the fourth order Runge-Kutta method. The mesh-independence with respect to time of finite volume schemes allows efficient coupling with computational fluid dynamics (CFD) tools. The accuracy and efficiency of the proposed method have been validated with analytically tractable and physically relevant fragmentation kernels and selection functions, demonstrating high accuracy in estimating number density functions and their integral moments. This new approach reduces computational time by approximately 60%, making it an excellent option for integration with CFD software due to its efficiency. |
| **35.** | An upgraded solid-phase assembly of chelators (DOTA and NOTA) enabled bacterial uptake studies of radiolabeled peptide<br>**B Pati**, A Kumar, **A Chowdhury, NM Tripathi, V Gour, A Mukherjee, A Bandyopadhyay** – ChemBioChem, 2024<br><br>**Abstract:** Among popular radio metal chelators, DOTA and NOTA have been remarkably considered in radionuclide therapy and imaging studies due to several advantages in pharmacology. Here, we developed a practical and general method for assembling DOTA and NOTA in the solid phase peptide (pseudo-dilute conditions) using a wide range of solvents with easily accessible and economical feedstocks, which mitigated unprecedented challenges associated with previously reported methods. This upgraded approach enabled an efficient installation of these two chelators on various bioactive peptide sequences. Finally, we assessed the antimicrobial activity of the DOTA- and NOTA-attached Combi peptides to B. subtilis, which was intact. The authenticity of the assembled DOTA framework was assessed by labeling $^{177}$Lu and in vitro bacterial uptake in E. coli and S. aureus. $^{177}$Lu-labeled DOTA-Combi peptide exhibited promising uptake for developing a bacterial infection imaging agent while negligible hemolysis activity even at >200 μM. This contribution will be valued for developing peptide radiopharmaceuticals with operational simplicity and economic approaches. |

| | |
|---|---|
| | 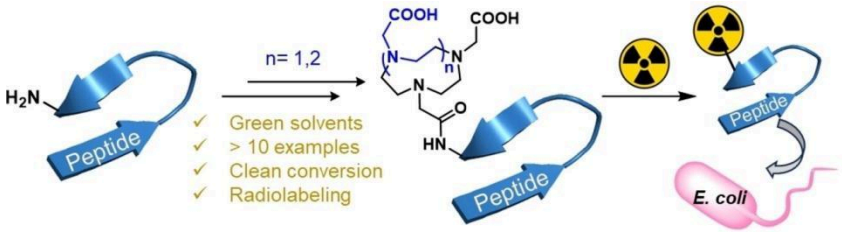 |
| **36.** | Antibacterial Lecithin/Chitosan nanoparticles for the sustained release of ciprofloxacin to treat ocular bacterial infections<br>**N Rasool, Y Thakur, Y Singh** - Chemistry–An Asian Journal, 2024<br><br>**Abstract:** Ocular drug-delivery is one of the most challenging areas owing to nature of ocular tissues. Various nanoformulations have been designed and investigated for drug-delivery to achieve high drug bioavailability. The major focus of preparations available in market is to utilize nanomaterial as drug-carrier, with less focus on developing functional-nanomaterials, which is a key knowledge gap in the field. To address this, we developed a nanoparticulate system from bioactive-polymers having intrinsic antimicrobial and mucoadhesiveness loaded with ciprofloxacin (cipro) to treat bacterial ocular infections. Cipro-loaded lecithin/chitosan nanoparticles were prepared and characterized for their physiochemical properties. They exhibited good drug loading efficiency and showed sustained drug-release for 72 h, with slow release for first 4 h followed by a burst release in phosphate buffered saline and simulated tear fluid. Cipro-loaded nanoparticles were assessed for their antibacterial potential against Staphylococcus aureus (96%) and Pseudomonas aeruginosa (72%) using optical density, disc-diffusion method, live-dead assay, and demonstrated promising antibacterial properties. The drug-loaded nanoparticles showed good cytocompatibility (~90%) towards murine fibroblasts and rabbit corneal cells. Being amphiphilic in nature, the nanoparticles exhibited mucoadhesiveness, haemocompatibility (<4%) and, thus, proving to be a promising candidate for treating ocular infections. This approach ensures efficient drug delivery and synergic/additive therapeutic effects. |
| **37.** | Assessing the geotechnical properties of lime-stabilized black cotton soil in the presence of nanosilica<br>K Bhavitha, P Gangavaram… **S Rohilla…** - International Journal of Geomechanics, 2024<br><br>**Abstract:** Expansive soils present substantial challenges in civil engineering because they undergo volume fluctuations with changes in water content, mainly affected by the clay mineral montmorillonite. Nanotechnology has rapidly and widely improved, finding applications across all engineering fields. This study focused on enhancing soil engineering performance using lime alone and the impact of varying quantities of nanosilica with lime in the soil, focusing on engineering parameters like Atterberg limits, maximum dry density, optimum moisture content, and unconfined compressive strength over curing periods of 7, 14, and 28 days. In this study, the basic properties of soil were initially determined. Then, lime was mixed with soil in different proportions of 2%, 4%, 6%, and 8% according to the dry weight of the soil. Based on strength criteria, soil mixed with 4% lime gives the best results. Keeping the lime content constant at 4%, nanosilica was added to the soil. These findings suggest modifications in the amended soil's plasticity, compaction characteristics, and strength with the minor addition of nanosilica to lime-mixed black cotton soil. The enhancement in strength of expansive soils relies on the amount of lime and nanosilica and the duration of curing. After conducting tests, it was found that the optimal quantities for lime and nanosilica through strength performance tests are 4% and 3%, respectively. The research asserts that adding nanosilica to lime notably improves the mechanical properties of black cotton soil. Scanning electron microscopy and X-ray diffractometer analyses support these findings, revealing variations in the character and strength |

| | |
|---|---|
| | of the CSH phase over curing time. These conclusions offer wide-ranging relevance for projects seeking to enhance the engineering properties of soft soils. |
| **38.** | Assessing the impacts of land use and climate change on streamflow generation in the Nowrangpur catchment based on the SWAT-land-use update tool<br>**S Kaur, SR Chavan** - Journal of Water and Climate Change, 2024<br><br>**Abstract:** Climate change and land-use change are two major factors that affect the hydrologic response of a river basin. The Soil and Water Assessment Tool (SWAT) is a reliable method to model the hydrology of a river basin. The SWAT-land-use update tool offers a user-friendly interface for the incorporation of dynamic land-use changes into hydrological modeling. This paper evaluates the impacts of climate and dynamic land-use changes on the streamflow generation in the Nowrangpur catchment encompassing Indravati dam, which is a major water resources project in India. Calibrating the SWAT model involved updating land-use data from 1985 to 2015, yielding satisfactory results. The future land-use/land-cover changes were predicted using the cellular atomata-artificial neural network model. Downscaled general circulation model data from 10 climate models were utilized to predict climate change impacts up to 2100. Projections indicate increased precipitation during the months from August to December with a more pronounced increase in the mid and far future. An uptrend in maximum and minimum temperatures for all months is observed in the far future relative to the baseline period. Furthermore, the streamflow predictions indicate a near-future decrease in total annual streamflow, followed by an increase of up to 41% in the mid and far future.<br> 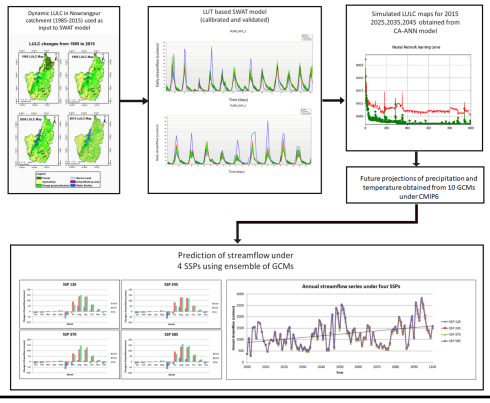 |
| **39.** | Bragg resonance in a two-layer fluid with the inclusion of current and tension at both surface and interface<br>**A Aggarwal**, SK Mohanty, **SC Martha** - Archive of Applied Mechanics, 2025<br><br>**Abstract:** In this study, the scattering of water waves by an undulating bottom in a two-layer fluid with current, surface tension, and interfacial tension is investigated. The perturbation technique followed by the Fourier transform technique are applied to solve the coupled boundary value problem. A Bragg resonance arises between the surface waves and the bottom ripples, which is associated with the reflection of incident wave energy. Hence, the Bragg coefficients namely, Bragg reflection and transmission coefficients, and associated velocity potentials are analysed which are obtained in integral forms. In order to clearly understand the efficacy of the present study, a certain type of undulating bottom, known as sinusoidal bottom undulation, has been examined. It has been shown that when the combined effects of surface tension, interfacial tension, and current are taken into account, the wave reflection is minimal. Moreover, a shift in the Bragg resonant frequency is seen with a change in current speed. In addition, interfacial tension influences both surface and interfacial waves, whereas surface tension primarily impacts surface waves. The results obtained here are expected to be qualitatively helpful in tackling problems of flexural gravity waves in two-layer fluid in the presence of current. |
| **40.** | B-tipping points in plankton dynamics: Stochasticity and early warning signals<br>**SN Chattopadhyay, AK Gupta** - Physical Review E, 2024 |

| | |
|---|---|
| | **Abstract:** Near a tipping point, a critical transition occurs when small changes in input conditions lead to abrupt, often irreversible shifts in a dynamical system's state. This phenomenon is observed in various biological and physical systems, including the collapse of species in ecosystems. Several statistical indicators, known as early warning signals (EWSs), have been developed to anticipate such collapses, garnering significant attention for their broad applicability. This paper investigates the stochastic versions of a bistable algae-zooplankton food-chain model under demographic and environmental noise. Our findings show that an increase in the predatory fish population, which consumes zooplankton, triggers a collapse in zooplankton abundance through a saddle-node bifurcation. Basin stability measure reveals that the resilience of the underexploited steady state significantly diminishes as the system approaches the collapse point. We evaluate the efficacy of various generic EWSs in predicting sudden collapses under both types of noise through statistical analysis. The robustness of AR(1) and variance are assessed through a comprehensive sensitivity analysis of processing parameters. We also calculate conditional heteroskedasticity, which minimizes false positive signals in the time series. Our results indicate that the prediction accuracy of variance and conditional heteroskedasticity remains independent of the noise type. However, AR(1) and skewness perform better in the presence of environmental noise. |
| **41.** | Damköhler number independent stable regime in reactive radial viscous fingering<br>**P Verma**, V Sharma, CY Chen, **M Mishra** - Journal of Fluid Mechanics, 2024<br><br>**Abstract:** The impact of a chemical reaction, A + B → C, on the stability of a miscible radial displacement in a porous medium is established. Our study involves a comprehensive analysis employing both linear stability analysis and nonlinear simulations. Through linear stability analysis, the onset of instability for monotonic as well as non-monotonic viscosity profiles corresponding to the same end-point viscosity are discussed and compared. We establish a ($R_b$, $R_c$) phase plane for a wide range of Damköhler number (Da) and Péclet number (Pe) into stable and unstable regions. Here, $R_b = \ln(\mu_B/\mu_A)$ and $R_c = \ln(\mu_C/\mu_A)$ and $\mu_i$ is the viscosity of fluid $i \in \{A, B, C\}$. The stable zone in the ($R_b$, $R_c$) phase plane contracts with increased Da and Pe but never vanishes. It exists even for Da → ∞. Interestingly, we obtain a Da independent stable region in the neighbourhood of $R_c = R_b$ where no transition occurs in stability despite changes in reaction rate. The study allows us to acquire knowledge about the transition of the stability for varying Da, Pe and different reactions classified using $R_b$, $R_c$.<br> 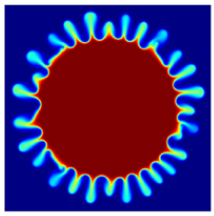 |
| **42.** | Deep learning at the forefront of detecting tipping points<br>**S Deb, PS Dutta** - Nature Machine Intelligence, 2024<br><br>**Abstract:** A deep learning-based method shows promise in issuing early warnings of rate-induced tipping, of particular interest in anticipating effects due to anthropogenic climate change. |
| **43.** | Dipeptide-functionalized type II heterojunctions: a bioinspired dual functionality for quinalphos detection and photodegradation<br>S Kalra, S Saini, N Kaur, **N Singh** - Journal of Materials Chemistry A, 2025 |

| | |
|---|---|
| | **Abstract:** Quinalphos, a widely used hazardous organophosphorus pesticide, is crucial in agriculture for safeguarding crops and improving yields. However, its persistent toxic residues result in environmental contamination and pose significant health hazards. Developing methods for the efficient degradation of quinalphos continues to be a major challenge. To address this issue, this study introduces the rational design of bioinspired dipeptide (DM2)-capped ZnO, forming type II staggered heterojunctions that utilize the synergistic interaction between DM2 and ZnO towards enhancing photocatalytic performance. This material enables efficient electron transfer due to the heterojunction structure, resulting in efficient photodegradation of quinalphos. The mode of interaction and photodegradation mechanism of quinalphos have been systematically studied, revealing a pseudo-first-order degradation kinetic model, with up to 99% removal efficiency. Degradation intermediates were identified using mass spectrometry analysis, and a comprehensive degradation pathway was proposed. This work highlights the potential of DM2-capped ZnO NPs as an effective and environmentally friendly material for the photodegradation of quinalphos, offering new avenues for sustainable environmental remediation. |
| **44.** | Dynamics of limit cycle oscillations in a multinozzle lean direct injection combustor<br>Y Nanda, A Saurabh, **L Kabiraj**, R Villalva Gomez, E Gutmark - AIAA Journal, 2024<br><br>**Abstract:** Thermoacoustic oscillations in a high-pressure multinozzle lean direct injection combustor with fuel staging have been examined. The combustor consists of three independently controlled fuel stages, i.e., the pilot, intermediate, and outer fuel stages. Limit-cycle oscillations have been identified for two cases with different fuel supplies to the three stages of the combustor, operating at different equivalence ratios. The oscillation dynamics of the two cases have been characterized and quantified by employing nonlinear time series analysis tools. Phase portraits, recurrence plots, and recurrence quantification methods were used by phase space reconstruction of the scalar pressure measurements. Further comparisons between the two cases were made by correlating the time-resolved OH* chemiluminescence images to the pressure oscillations. Phase averaging and spectral proper orthogonal decomposition were used to understand the flame dynamics between the three fuel stages. |
| **45.** | Effect of functionalization on properties of Scandium-based MXenes: A DFT study<br>**A Pandey, N Sardana** - Computational Materials Science, 2025<br><br>**Abstract:** This study investigates the impact of functionalizing OH, F, Cl, and Br on the dynamical stability, mechanical, electronic, and optical characteristics of two-dimensional Sc-based $Sc_2XZ_2$ MXenes (X = C, N, and Z = OH, F, Cl, and Br) by density functional theory (DFT) simulations. The findings reveal that surface functionalization significantly affects the vibrational, electronic, and mechanical characteristics of the MXene. Functionalization enhances the mechanical properties of Sc-based MXene. Functionalization on $Sc_2C$ transforms them into semiconductor materials except Sc-based pristine MXene and $Sc_2NZ_2$ (Z = OH, F, Cl, Br). Furthermore, the dielectric characteristics of these MXenes are also affected by the nature of surface functionalization. Our calculations demonstrate that semiconductor MXene systems with larger band gaps exhibit higher Seebeck coefficient values at the same temperature compared to other MXenes. These results have potential applications in the design of optoelectronic and nanoelectronics devices.<br> 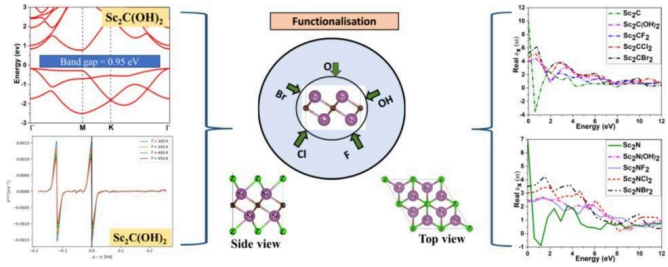 |

| | |
|---|---|
| **46.** | Efficacy of carbon nanotube bucky paper for interlaminar damage sensing in composites and fiber-metal laminates<br>**V Kumar, PK Agnihotri** - Polymer Composites, 2024<br><br>**Abstract:** Delamination between adjacent laminas and debonding at the fiber/metal interface are common failure modes in composites and fiber-metal laminates (FMLs). During the initial stages, these flaws are difficult to detect because of their small size and limited applicability of existing damage-sensing techniques due to the associated heterogeneity and anisotropy with composites and FMLs. Here, we demonstrate a feasible interlaminar damage-sensing strategy in composites and FMLs using carbon nanotube (CNT) bucky paper (BP). The microstructure dependence of BP electrical conductivity allows it to sense the damage under varying loading conditions. The accuracy of strain sensing with BP is similar to the commercial 120 Ω strain gauge. The BP sensor accurately detects the interlaminar damage in composites (glass fiber/epoxy, carbon fiber/epoxy) and glass fiber–Al (GLARE) laminates. The delamination is marked by a steep rise in the electrical resistance of BP-modified coupons. Moreover, the sensing capability of the BP sensor is found to be independent of the electrical conductivity of the tested coupons. Thus, the present approach is applicable to sense the interlaminar damage in a much wider class of structural composites and FMLs.<br>Highlights:<br>● Timely and accurate damage detection in composites is important to ensure their structural integrity.<br>● Electrical resistance of bucky paper (BP) varies with deformation.<br>● Performance of the BP sensor is comparable to the strain gauge at small strains.<br>● BP accurately captures interlaminar damage in composites and FMLs.<br>● BP is suitable for damage sensing in a wider class of layered materials. |
| **47.** | Employing mesoporous nitrogen containing carbon for simultaneous electrochemical detection of heavy metal ions<br>**N Bhatia, D Mehta, K Garg, S Kaur, T C. Nagaiah** - Chemistry–An Asian Journal, 2024<br><br>**Abstract:** Heavy metal ions are major contributors to water pollution, posing significant threats to both ecological balance and human health due to their carcinogenic properties. The increasing need for heavy metal detection highlights the advantages of electrochemical methods, which offer high sensitivity and efficiency. Herein mesoporous nitrogen containing carbon (MNC) was utilized for the simultaneous determination of heavy metals using square wave voltammetry technique in the established conditions of a buffer pH of 5.0. MNC demonstrated low detection limits (1, 10 and 50 μM), wide linear ranges (1 μM - 6 mM, 10 μM - 7 mM and 50 μM - 17 mM), and high sensitivities (2.5 μA μM-1 cm-2, 1.03 μA μM-1 cm-2 and 5.14 mA mM-1 cm-2) for, $Pb^{2+}$, $Cd^{2+}$ and $Cu^{2+}$, respectively. Moreover, the reproducibility, and selectivity of the sensor was investigated in the presence of K+, Mg2+, Zn2+, Ni2+, and Fe3+ which are the possible interferents present in water. |
| **48.** | Enhanced catalytic degradation of methylene blue using self-propelled Janus micromotors: An insight into decomposing characteristics of passive and active hematite particles studded with Pt nanoparticles<br>**F Khan, VS Pawak**…**T Mondal, M Sabapathy** - The Journal of Chemical Physics, 2024<br><br>**Abstract:** Recent advancements in catalytic micromotors have shown significant potential for environmental applications, yet challenges such as particle agglomeration persist. In this study, we compare the degradation of methylene blue using hematite particles fully coated with platinum and those partially decorated with platinum. The selective decoration, confirmed through techniques like EDX, FESEM, TEM, and XPS, plays a crucial role in the micromotors' behavior. The decomposition of hydrogen peroxide ($H_2O_2$) by Pt nanoparticles on one side of the |

| | |
|---|---|
| | hematite particles generates thrust, propelling the micromotors and enhancing their interaction with pollutant molecules. This active mobility helps counteract agglomeration, preventing the formation of irregular 3D clusters and improving catalytic efficiency. Our findings show that partially decorated particles achieve up to 85% dye removal within 90 min, outperforming fully decorated particles, which reach only 33% efficiency due to aggregation and sedimentation. These results underscore the importance of optimized surface decoration for improving the performance and stability of catalytic systems in pollutant degradation. |
| **49.** | Enhancing N-V−-center coherent emission using the weak-coupling regime of a hybrid metal-dielectric architecture<br>**N Singh**, D Sehgal, A Venkatesan, **RV Nair** - Physical Review Applied, 2024<br><br>**Abstract:** Negatively charged nitrogen-vacancy (N−$V^-$) centers in diamonds have rapidly developed due to their exceptional quantum optical and spin properties at room temperature. However, their applicability is limited by broad phonon-sideband emission with feeble coherent emission at the zero-phonon line (ZPL). This calls for the exploration of photonic cavities to enhance ZPL emission. We propose an easy-to-fabricate hybrid metal-dielectric nanocavity with low mode volume to enhance ZPL emission while suppressing phononic emission channels due to different N−$V$ charge states. We find a 400% enhancement in the emission rate and outcoupling of emitted light at the ZPL with better directivity by deterministic positioning of the N−$V^-$ inside the nanocavity, corroborated by numerical simulations. The pump-dependent measurements confirm better emission saturation intensity for the cavity-coupled N−$V^-$s. The proposed tunable nanocavity structure can be applied to a broad range of quantum emitters to control their emission so that their use in quantum technologies could be improved. |
| **50.** | Enhancing solar thermal fuel efficiency through dopant-mediated structural modifications in triphenylene-based mesogenic matrices<br>**Ashy**, K Banerjee, **M Gupta** - ACS Applied Energy Materials, 2024<br><br>**Abstract:** Solar thermal energy storage (STES) presents a promising solution for overcoming the challenges associated with intermittent solar energy capture and storage. By harnessing concentrated solar heat to photothermal energy conversion, solar thermal fuels (STFs) offer a unique approach for achieving long-term energy storage and on-demand energy delivery. Addressing this, we investigated the incorporation of discotic nematic hexa-azobenzene-functionalized triphenylene (TPAB) into columnar hexagonal self-assemblies of hexa-alkoxytriphenylene (TP) liquid crystal (LC) matrices to improve STF efficiency. By variation of the dopant concentration, the impact on energy storage and release properties is explored. X-ray diffraction (XRD) analysis unveils a correlation between the dopant concentration and LC packing, indicating disruption of the ordered structure at higher concentrations. Polarized optical microscopy (POM) images indicate a transition from an ordered columnar hexagonal ($Col_h$) mesophase to isotropic phases in *cis*-rich films with increasing dopant concentration, influencing heat release behavior. Experimental findings demonstrate that optimal heat release occurs at specific dopant concentrations like 1.5 wt % for **1a** and 1 wt % for **2a** due to the interplay of isomerization and lattice enthalpy. The heat release dynamics were observed in both green light emitting diode (LED) and direct sunlight-charged thin films. These insights contribute to understanding dopant-mediated enhancements in STF performance, offering valuable guidance for advancing the creation of next-generation STES systems. |

| | |
|---|---|
| | 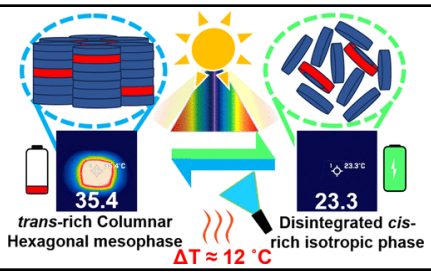 |
| **51.** | Exploring algorithmic solutions for the Independent Roman Domination problem in graphs<br>**K Paul, A Sharma, A Pandey** - Discrete Applied Mathematics, 2025<br><br>**Abstract:** Given a graph G=(V,E), a function f:V→{0,1,2} is said to be a Roman Dominating function if for every v∈V with f(v)=0, there exists a vertex u∈N(v) such that f(u)=2. A Roman Dominating function f is said to be an Independent Roman Dominating function (or IRDF), if $V_1 \cup V_2$ forms an independent set, where $V_i=\{v \in V \mid f(v)=i\}$, for $i \in \{0,1,2\}$. The total weight of f is equal to $\sum_{v \in V} f(v)$, and is denoted as w(f). The Independent Roman Domination Number of G, denoted by $i_R(G)$, is defined as min{w(f)\|f is an IRDF of G}. For a given graph G, the problem of computing $i_R(G)$ is defined as the Minimum Independent Roman Domination problem. The problem is already known to be NP-hard for bipartite graphs. In this paper, we further study the algorithmic complexity of the problem. In this paper, we propose a polynomial-time algorithm to solve the Minimum Independent Roman Domination problem for distance-hereditary graphs, split graphs, and $P_4$-sparse graphs. |
| **52.** | Exploring the role of spirituality and environmental concern on millet purchase intention<br>KB Gupta, **A Bhardwaj** - Metamorphosis, 2024<br><br>**Abstract:** The present study explores the impact of spirituality and environmental concerns on the purchase intention of Indian consumers through an extended version of the Theory of Planned Behaviour (TPB). Based on the data collected from 448 people, Partial Least Square Structural Equation Modeling (PLS-SEM) is used to develop and test the proposed model. The present study confirms the positive impact of attitude, subjective norms, and perceived behaviour control on the purchase intention of millet products. The study also confirms the importance of spirituality and environmental concerns on the intention to purchase millet products. Since millet is a nutrient-dense and climate-resilient crop, the findings advocate for the government and business organizations to promote millet products on these dimensions. With the increased awareness of the importance of environmental sustainability and spirituality, the present study provides a new dimension of research and managerial action. |
| **53.** | Hazard, and risk modelling of glacial lakes in the Sikkim Himalaya: Integrating qualitative and quantitative approaches for hazard assessment<br>**D Gaikwad, RK Tiwari, M Kumar, S Guha** - Geomorphology, 2024<br><br>**Abstract:** Glacial lakes are prone to outburst due to breaching or overtopping of natural dams, leading to Glacial Lake Outburst Floods (GLOFs). These floods represent a substantial danger to communities downstream and essential infrastructure. To address this issue, it is crucial to investigate certain key factors, including gaining insight into the dynamics of glacial lakes, identifying dangerous ones, and assessing the associated level of risk. In this study, we scrutinized the temporal changes of glacial lakes in the Sikkim Himalaya for the years 1990, 2000, 2010, and 2020 using Landsat satellite imageries. Furthermore, we performed a hazard assessment of GLOFs in terms of both qualitatively, and quantitatively assessment. Moreover, qualitative evaluation involves seven external triggers and quantitative assessment employed by utilizing the Fuzzy Analytical Hierarchy Process (FAHP) method, considering six causative factors. Finally, we modelled the degree of risk associated with glacial lakes by quantifying downstream impacts with the help of GIS-based Stochastic Inundation Monte-Carlo Least Cost |

| | |
|---|---|
| | Path model (MC-LCP). The findings revealed that the number of glacial lakes increased from 309 to 440, with a total area expansion from 22.83 $km^2$ to 30.71 $km^2$ over the 30-year period. Also, among the 51 glacial lakes susceptible to GLOFs, seven lakes were classified as highly hazardous and another six were deemed to pose high risk. Overall this study contributes to planning field investigations and developing effective mitigation strategies to minimize the significant socio-economic losses caused by GLOFs in the Sikkim Himalaya.<br> 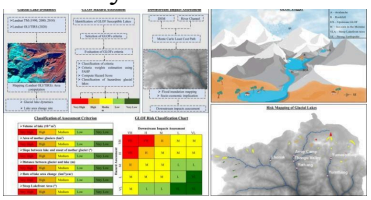 |
| **54.** | HeRo: Heuristic-based routing in payment channel networks<br>**S Mishra, V Aggarwal, S Pal, V Agarwal** - IEEE Networking Letters, 2024<br><br>**Abstract:** Payment channels support off-chain transactions by enhancing transaction speed and reducing fees in the main blockchain. However, the costs and complexity of the network increase as we increase the size of the network. To address these challenges, we propose Heuristic-Based Routing with Scheduling (HeRo) combining heuristic-based routing and scheduling techniques in Payment Channel Networks (PCNs). HeRo achieves a cost reduction of 32.71% and 73.08% compared with multi-charge PCN (MPCN-RP) and Dijkstra algorithms, respectively. |
| **55.** | Impact of angle-dependent magnetic fields on crack dynamics and particle ordering in drying colloidal droplets<br>**D Rani**, SK Saroj, **S Sarkar** - Colloids and Surfaces A: Physicochemical and Engineering Aspects, 2024<br><br>**Abstract:** We present an experimental study that unveils the intricate interplay between desiccation crack patterns and hematite ellipsoidal nanoparticle alignment under the influence of inclined magnetic fields. Through experimental observations, we demonstrate how a magnetic field oriented between 0◦ and 90◦ in the polar axis leads to significant transitions in crack patterns on the substrate plane. Our findings reveal that the ellipsoidal nanoparticles align with their minor axes along the tensile stress direction generated while crack propagation at specific locations on the edges within the deposits. Depending on the magnetic field orientation and the location, hook-shaped cracks at the nanoscale are observed in addition to the commonly observed circular and straight ones. Complementary simulation studies illustrate the changes in magnetic flux vector configurations at the top and base of the sessile droplet in the x–y plane, corresponding to the applied field direction. These results correlate with magnetic torque calculations, which show that the azimuthal component of the ellipsoids' magnetic moment significantly influences particle alignment during the self-assembly process. This work provides critical insights into the fundamental mechanisms underlying the close coupling between desiccation cracking, nanoparticle alignment, and magnetic field directions. Our results show potential usage in nanotechnology and inkjet printing associated with microfluidics, where multicomponent desiccation of microdroplets containing anisotropic nanoparticles occurs in the presence of external forces.<br> 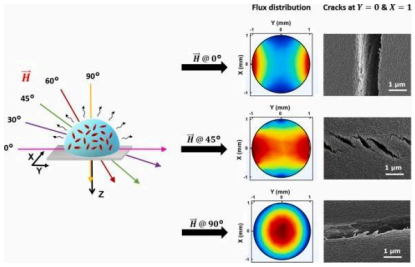 |

| | |
|---|---|
| **56.** | Interface engineering for minimizing trapped charge density in β-$Ga_2O_3$ Schottky barrier diodes for high-performance power devices<br>**Shivani**, AG Chakkar, P Kumar, **M Kumar** - Materials Today Physics, 2025<br><br>**Abstract:** Gallium oxide ($Ga_2O_3$), with its ultra-wide bandgap and high breakdown voltage, has emerged as a leading candidate for next-generation power devices. The performance and the Baliga figure-of-merit for power devices critically depend on breakdown voltage sustained by Schottky contact of metal with ultra-wide gap materials. However, high-quality Schottky contacts with $Ga_2O_3$ presents a significant challenge due to the presence of surface defects and formation of metal induced mid-gap defects states in $Ga_2O_3$. In this study, we investigate the electrical properties and defects at the interface between Ni metal and β-$Ga_2O_3$ thin films. Additionally, a 20 nm MgO thin films with various oxygen contents were deposited on β-$Ga_2O_3$ using radio-frequency magnetron sputtering and Ni/MgO/β-$Ga_2O_3$ metal-insulator-semiconductor Schottky diodes were fabricated. The frequency dependent C-V characteristic and surface-sensitive XPS depth profile is employed to study the interface of Ni/$Ga_2O_3$ and Ni/MgO/$Ga_2O_3$ Schottky barrier diodes. Our results show that the Ni/MgO/$Ga_2O_3$ Schottky barrier diode with 66 % $O_2$ in the MgO thin film during synthesis attains a barrier height of 0.87 eV. Subsequent post-metallization annealing at 300 °C in an Ar ambient for 30 min enhances the barrier height up to 1.1 eV. Also, a reduced on-resistance of 11.65 mΩ $cm^2$ and a lower on-voltage of 0.3V was obtained after annealing in Ar. The frequency dependent C-V characteristic results show no dispersion in capacitance for the annealed sample which signify the passivation of interface defects density ($\Delta_{it}$) and oxide charges density ($N_f$) in the dielectric layer (MgO). The minimum value of $D_{it}$ and $N_f$ achieved for the sample having highest barrier height (1.1eV) are 5.41 × $10^{11}$/eV/$cm^2$ and 2.91 × $10^{10}$/$cm^3$, respectively. This study establishes a vigorous foundation for the expanded utilization of $Ga_2O_3$ in power electronics devices, emphasizing the vital role of interface engineering. |
| **57.** | Internal gas injection into ladle shroud and improvement in tundish hydrodynamic performance<br>**A Maurya, PK Singh** - Steel Research International, 2024<br><br>**Abstract:** In this article, two-phase experimental and numerical investigations are performed to study the effect of inert gas injection to ladle shroud on the hydrodynamic performance of tundish. It is widely known that the flow of molten steel through a shroud, with or without inert gas injection, can influence the flow behavior in the tundish and, consequently, the hydrodynamic performance. However, large throughput rates may promote refractory wear, slag entrainment, and large tundish eye, which are known to seriously impair steel cleanliness, implying a severe need for optimization of the inert gas injection rate into the ladle shroud. In this study, two distinct reduced scale slab-casting tundishes (from different plants) with scale factors of 0.35 and 0.40 fitted with various flow modifiers are considered. Experiments are performed considering gas-to-liquid loading ratios of 10, 20, and 30%. An improved tundish hydrodynamic performance is observed during the experiments, which is validated with numerical modeling results using ANSYS Fluent 2021R1. Although gas injection to the shroud certainly enhances the hydrodynamic performance of tundishes, the effect fades away beyond 20% of the gas-to-liquid loading ratio, regardless of the tundish design, capacity, and different flow modifiers used. |
| **58.** | Lanthanide-Tetradentate Schiff base-PMMA composite films for tunable white light emission<br>U Sarkar, M Singh, **MK Adak**, S Bhattacharya - Advanced Optical Materials, 2024<br><br>**Abstract:** Multicolor emissive Schiff base lanthanide Poly(methyl methylacrylate) [PMMA] composite films are fabricated for white light generation. Three isostructural lanthanides (III) complexes [$Eu^{III}_2(L)_2(NO_3)_2(dmf)_2$ (**1**), $Tb^{III}_2(L)_2(NO_3)_2(dmf)_2$ (**2**) and $Gd^{III}_2(L)_2(NO_3)_2(dmf)_2$ (**3**)] are synthesized, characterized from the ligand obtained by 1:1 condensation of salicylaldehyde and 2-(2-Aminoethoxy)ethanol, $H_2L$. The photoluminescent studies revealed pure blue, green, |

| | |
|---|---|
| | and red color emissions from $Gd^{III}L$, $Tb^{III}L$, and $Eu^{III}L$ complexes, although the central metal centers have identical dodecahedron geometry. Intensified ligand emission is attested for the blue emitter-$Gd^{III}L$ complex while the "antenna effect" is witnessed for green $Tb^{III}L$ and red $Eu^{III}L$ complexes. Co-doping these multicolor luminescent emitters into the PMMA polymer the intensity of luminescence improved. A conscientious combination of red-$Eu^{III}L$ with green-$Tb^{III}L$ *Lanthanide metal Schiff base complexes* in a specified concentration, distinct white light is accomplished for the *first time* with Commission Internationale de I'Éclairage (CIE) values of 0.33, 0.30, very close to the ideal white emitter. The newly developed lanthanide-Schiff base-PMMA composite films are transparent and highly desired materials in optoelectronics, microscopy, and sensing. |
| **59.** | Mammoth backlog of court cases pending in India: A spatial visualization<br>S Agarwal, **SR Behera** - Regional Studies, Regional Science, 2024<br><br>**Abstract:** The judiciary plays a pivotal role in maintaining the rule of law and protecting the fundamental rights of citizens, pledging the efficient enforcement of rules and regulations and upholding civil and criminal justice in principles. The judicial system in an emerging economy like India must ensure timely and equitable justice for all citizens. For more than the last thirty years, the Indian judiciary has been facing colossal pendency levels and long case processing times. Against this backdrop, this paper visualises the spatial variations in the number of unresolved court cases in different districts of India in 2023. The spatial visualisation using a cartogram map elucidates some specific districts in certain Indian states, based on their population, that are now awaiting huge court proceedings. The spatial variations in pending cases across different regions emphasise the need for deliberate initiatives to promote regional justice by maximising the number of pending cases to be disposed of as soon as possible. The visualisation analysis validates that for the smooth functioning of overburdened pending court proceedings and to maximise the number of cases disposed, the judicial system needs substantial reforms, upgradation of massive court infrastructure, required reallocation and recruitment of judges and court staff, especially in high-density populated areas like New Delhi and Mumbai metropolitan cities in India. Therefore, this finding suggests that a massive backlog of pending court and overburdened cases knowledge is critical for state governments seeking to increase judicial efficiency by focusing on districts with a high volume of pending cases. |
| **60.** | Mitigation of hydroelastic responses of a very large floating structure by flexible porous barriers<br>S Singla, **SC Martha**, T Sahoo - Proceedings of the Institution of Mechanical Engineers, Part M: Journal of Engineering for the Maritime Environment, 2024<br><br>**Abstract:** The role of a vertical flexible porous barrier of two different configurations, namely (i) surface-piercing barrier (SPB) and (ii) bottom-standing barrier (BSB) in the mitigation of hyroelastic responses of a very large floating structure (VLFS) is analysed. Both the flexible barrier and the floating plate are modelled using Euler-Bernoulli beam equation under the assumption of small amplitude structural response. The solution of the associated mathematical problem is obtained using the eigenfunction expansion method. Various results illustrating the effect of the barrier length, porous-effect parameter, and the barrier-VLFS spacing on various hydroelastic responses of the VLFS are presented. Moreover, results on barrier deflection and overturning moments of the flexible porous barrier for various structural parameters are presented. Energy identity is derived using Green's identity and used to check the accuracy of the computational results. The study reveals that for suitable values of the structural flexibility, porosity and barrier configurations, wave-induced structural responses on the VLFS and barriers can be reduced significantly. Moreover, the study depicts that the presence of flexible porous barriers can significantly reduce the wave reflection and wave forces exerted on the floating elastic plate. |
| **61.** | Morphing evaporative heat and mass transport of nanofluid droplets by electric field |

| | |
|---|---|
| | P Dhar, **A Chattopadhyay**, DK Agarwal - Experimental Thermal and Fluid Science, 2024<br><br>**Abstract:** In this research, evaporation behaviour of pendant droplets of stable nanocolloidal dispersions in the presence of an electric field is probed, both experimentally and theoretically. It is observed that the colloid droplets evaporate faster than their water counterparts in absence of the field. But within field environment, increase of electric field strength suppresses the evaporation rates, while the field frequency shows no appreciable effects on the evaporation rates. Also, the reduction of evaporation rate in field environment is pronounced at higher colloidal concentrations. Theoretical analyses from existing models reveal that neither alterations in the surface tension nor the diffusion-driven classical evaporation model can map the reduced evaporation rates. Through infrared thermography and Particle Image Velocimetry, reduction of internal thermo-solutal circulation velocity for the droplet is noted when stimulated by the electric field, which is shown to directly affect the rate of evaporation. The effects of electrohydrodynamic advection, electro-thermal and electro-solutal convection on the evaporation behaviour is modelled by a scaling approach. The influence of dominant non-dimensional numbers, such as thermal Marangoni number, solutal Marangoni number, electro-Prandtl number, electro-Schmidt number, and the Electrohydrodynamic number, are quantified and discussed. Stability considerations reveal that the stable internal flow behaviour is retarded by the electric body force, with the reduction via the electro-solutal route being predominant, and the internal flow velocities being mapped well by the electro-solutal model. The findings may hold implications in the domain of multiphase transport phenomena of complex fluids at micro and macroscales. |
| **62.** | Multi-scale inferomedial femoral neck bone quality in type 2 diabetes patients with fragility fracture<br>**P Sihota, S Kumar**, R Dhaliwal, **P Uniyal**, **RN Yadav**, V Dhiman, D Neradi, S Karn, M Sapara, S Sharma, S Aggarwal, V G Goni, V Mehandia, B Busse, D Vashishth, S K Bhadada, **N Kumar** - Bone, 2024<br><br>**Abstract:** Both trabecular and cortical bone undergo changes at multiple scales. We previously demonstrated the multi-scale changes in trabecular bone quality that contribute to bone fragility in type 2 diabetes (T2D). The link between increased fragility in T2D and multi-scale changes in cortical bone and their interaction with glycation remains unclear. This study presents, first-ever, multi-scale cortical bone quality parameters in T2D patients after their first hip fracture. The study objective was to determine the association between cortical porosity (Ct.Po.), mechanical, material, and bone compositional properties in T2D. Inferomedial femoral neck (FN) bone tissue specimens were collected from patients ($n = 10$ with T2D, $n = 25$ age- and sex-matched non-diabetes controls) who underwent hip replacement surgery following the first hip fragility fracture. Bone mineral density at FN was found to be similar between groups. In T2D, Ct.Po was higher ($p = 0.038$), while ultimate stress ($p = 0.021$), ultimate strain ($p = 0.040$), post-yield strain ($p = 0.011$), toughness ($p = 0.005$), yield energy ($p = 0.003$), and post-yield energy ($p = 0.004$) were notably lower. Tissue compositional differences included lower gravimetric mineral/matrix ($p = 0.017$), higher non-enzymatic collagen cross-link ratio (NE-xLR) ($p = 0.049$) and higher sugar/matrix ratio ($p = 0.042$) in T2D. Fluorescent advanced glycation end-products (fAGEs) content was higher in T2D bone ($p = 0.043$). At the mesoscale, the fAGEs in the bone matrix are inversely related to the yield- and ultimate strain of T2D bone, and NE-xLR is negatively correlated with yield- and ultimate- stress in the T2D group. In conclusion, study findings demonstrate that elevated glycation weakens the mechanical integrity of cortical bone by reducing its ability to absorb energy and resist deformation, thereby contributing to bone fragility in T2D. The strong association of fAGEs with lower yield strain, along with the association of NE-xLR with lower yield- and ultimate stress, establishes a causal link between AGEs and the deterioration of cortical bone mechanical properties. These findings underscore the need for strategies targeting glycation and collagen quality to mitigate fracture risk in T2D patients. |

| | |
|---|---|
| **63.** | [Nanoporous gold films as a perfect NIR–UV absorber](#)<br>**J Singh**, A Chopra, SS Pal, **S Sarkar** - Applied Surface Science, 2024<br><br>**Abstract:** Materials with wide and high absorptivity bandwidths are increasingly essential in various applications such as solar energy harvesting, photodetection, and thermal emission. This study aims to discover a new cost-effective, and scalable fabrication method for achieving near-ideal broadband light absorbers. Here, we demonstrate that a nanoporous gold (NPG) film serves as an extreme example of an optical absorber material in the NIR–UV region. The absorption bandwidth can be systematically engineered by adjusting the thickness, fractal dimension and filling factor of the NPG films. These films exhibit full absorption bandwidth with absorbance ~0.85 for wavelengths in the UV–Vis-NIR regimes. To validate our findings, we developed a numerical model using the finite-difference time-domain (FDTD) method combined with a hybrid effective medium approach. The simulations reveal that the observed increase in absorption is primarily due to localized surface plasmon resonance (LSPR) occurring within the gaps of the porous structures. Manipulation of the thickness of the NPG film allows for spectral tunability of the resonance peak position of the LSPR on the absorption spectrum, thus optimizing the broadband absorption. These findings underscore the potential of NPG as a versatile material for engineering broadband light absorbers with tunable properties, offering promising avenues for applications in thermal emission, photodetection, and solar energy harvesting.<br> 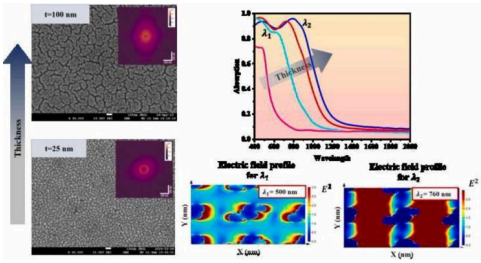 |
| **64.** | [NVMS-Net: A novel constrained noise-view multi-scale network for detecting general image processing based manipulations](#)<br>G Singh, **K Rana, P Goyal**, S Kumar - IEEE Transactions on Artificial Intelligence, 2024<br><br>**Abstract:** Ensuring the authenticity and integrity of digital images is a major concern in multimedia forensics, driving research on universal schemes for detecting diverse image manipulations (or processing operations). Although some prior works have addressed general-purpose image manipulation detection, they have been evaluated under constrained environments. Developing an approach that effectively identifies multiple manipulations in real-world scenarios remains a challenge. To address this issue, in this paper, we have designed a novel constrained Noise-View based Multi-Scale Network (NVMS-Net) that jointly exploits constrained noise-view and multi-scale feature learning for multiple image processing operation detection. Our NVMS-Net includes four stages: constrained noise-view, generalizable feature learning, multi-scale feature learning, and classification. Firstly, a Noise Extraction Layer (NEL) is employed to suppress the image content information for the extraction of noise features. The statistical modeling of these noise features is further improved by Statistical Modeling Layer (SML) to achieve a better noise-view of image tampering artifacts. Then, we use multiple CBR blocks to learn generalizable noise features that are sensitive to image manipulations. Further, a Multi-Scale Aggregation Module (MSAM) is proposed that leverages image tampering features at multiple scales through the aggregation of low and high-level features. The extensive experimental results show that the NVMS-Net consistently outperforms the existing approaches on different dataset settings. Importantly, NVMS-Net shows better performance in real-world scenarios, particularly against anti-forensic techniques and adversarial attacks. The proposed |

| | |
|---|---|
| | NVMS-Net provides an overall accuracies of 98.21% and 98.60% on BOSSBase and Dresden datasets, respectively. |
| **65.** | On the importance of the metal catalyst layer to the performance of CNT-based supercapacitor electrodes<br>K Chatterjee, V Kumar, **PK Agnihotri**… - IEEE Transactions on Nanotechnology, 2024<br><br>**Abstract:** The power and energy densities of a Supercapacitor (SC) is largely dictated by the accessibility of the nano-porous area of the electrode to the electrolyte ions. Carbon nanotubes (CNT) have high electrical conductivity, and more importantly, may be grown into architectures with high surface area. However, this is not easy to achieve in practice. CNT electrodes are fabricated by chemical vapor deposition (CVD), after a metal catalyst layer is coated on a current collector. In this work, the control of the metal catalyst layer, by varying the dip-coating time and CVD process parameters, is shown to be crucial to pore morphology and consequent SC performance. The dip-coating time is adjusted to obtain thin and uniform coating. Further, optimum reduction of the nickel layer with hydrogen is required to produce thin CNTs with adequate inter-tube separation that facilitate ion accessibility within the pores. The height of the CNT forest is also optimized to prevent decrease in specific capacitance due to reduced accessibility. Proper optimization of the process parameters results in a pore morphology conductive to ion diffusion, and simultaneous improvement in energy and power density. |
| **66.** | Origin of the suppression of magnetic order in MnSi under hydrostatic pressure<br>P Dalmas de Réotier, A Yaouanc, D Andreica, **R Gupta**, R Khasanov, G Lapertot - Physical Review Letters, 2024<br><br>**Abstract:** We experimentally study the evolution of the magnetic moment m and exchange interaction J as a function of hydrostatic pressure in the zero-field helimagnetic phase of the strongly correlated electron system MnSi. The suppression of magnetic order at ≈1.5 GPa is shown to arise from the J collapse and not from a quantum fluctuations induced reduction of m. Our work provides benchmarks for first principles theories that are challenged by the presence of strong correlations and the possible role of Hund's coupling. In addition, our experimental data are consistent with a reorientation of the magnetic propagation wave vector recently evidenced above ≈1.2 GPa. This result calls for a thorough investigation of the crystal structure in this pressure range. |
| **67.** | Oxidation behavior of mechanically alloyed high-entropy alloys: A review<br>SM Dikonda, **A Anupam**, M Vaidya - Advanced Engineering Materials, 2024<br><br>**Abstract:** High-entropy alloys (HEAs) owing to their entropy maximized design exhibit simple solid solution structures and possess fascinating properties. In addition to mechanical properties, the oxidation resistance is an important property that is crucial for determining the suitability of high-temperature operation of the structural members. Among processing routes, mechanical alloying is one of the most widely used techniques primarily due to the generation of nanocrystalline grains and alloying elements with wide melting point differences. Mechanically alloyed HEAs differ from cast alloys in several aspects, including the phases developed, microstructure, oxidation products, and mass gain kinetics. This difference is largely attributed to the presence of numerous grain boundaries in mechanically alloyed HEAs, which serve as significant diffusion paths. This article aims to provide a comprehensive overview of oxidation studies performed in several mechanically alloyed HEAs, detailing their microstructure, oxidation products, and kinetics. It also compares the oxidation behavior of few of these systems with their cast counterparts. The oxidation behavior is further analyzed from both thermodynamic and kinetic perspectives. Finally, the article suggests several future research directions that can further the understanding of oxidation behavior of mechanically alloyed HEAs and contribute to their development. |

| | |
|---|---|
| **68.** | Phase transitions in a multi-phase lattice hydrodynamic area occupancy model in mixed disorder traffic considering connected and human-driven vehicles<br>M Verma, **AK Gupta**, S Sharma - Physica A: Statistical Mechanics and its Applications, 2025<br><br>**Abstract:** Recent developments in transportation systems have significantly accelerated the emergence of connected vehicles (CVs) within the V2V environment, coexisting with human-driven vehicles (HDVs). Understanding the traffic dynamics in the mixed environment of CVs and HDVs in disordered traffic where the vehicles do not follow lane discipline becomes excessively complex. In this context, a lattice hydrodynamic model is proposed that incorporates the area occupancy effect for the mixed traffic environment. Further, a multi-phase optimal velocity function is considered to portray the traffic flow characteristics more realistically as it considers the discontinuous accelerations occurring in real traffic. The traffic flow behavior is investigated through linear stability analysis, which depicts that the stability region narrows down as the fraction of CVs increases. Moreover, the mKdV equation is attained to study the slowly varying behavior of density waves near the critical point. It is observed that with an increase in the fraction of CVs, traffic flow stability increases significantly with increasing sensitivity. Notably, the theoretical results are validated through numerical simulation on unidirectional multi-phase traffic flow. |
| **69.** | Photoresponsive ionic liquid crystals<br>**Ashy, M Gupta** - Journal of Molecular Liquids, 2024<br><br>**Abstract:** Photoresponsive ionic liquid crystals (PILCs) emerge as a captivating class of materials, seamlessly merging the distinct properties of ionic liquids, liquid crystals, and photoresponsive groups. This innovative combination empowers PILCs to exhibit remarkable phase transitions and responsiveness to external stimuli, particularly light and temperature. In this review, we have detailed various kind of PILCs reported to date. PILCs are further categorized based on their molecular composition. One-component PILCs are composed of a single component having ionic, photoresponsive and mesogenic groups. They are further subdivided into monomeric, oligomeric, and polymeric one-component PILCs. Monomeric PILCs exhibit lyotropic (concentration-dependent) and thermotropic (temperature-dependent) structural changes in response to external stimuli. Oligomeric PILCs, with multiple photoresponsive units, offer precise control over self-assembly and phase behavior. Polymeric PILCs feature a polymeric cationic backbone with attached anionic photochromic groups. Furthermore, two-component PILCs consist of two distinct components consisting of varying combination of ionic, photoresponsive and mesogenic groups. Similarly, three-component systems consist of three distinct components of similar varying combination as discussed above. All these materials enable precise control of phase transitions and structural properties through light stimuli, opening up exciting possibilities for future innovations in optoelectronic devices, smart sensors, and light-controlled systems.<br> 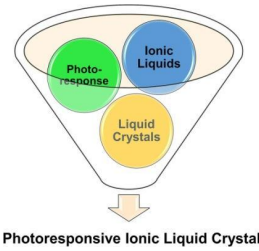 <br> |
| **70.** | Production of metallic foam and its behavior at different strain rates: A review<br>Avinash, M Mursaleen, **N Kumar** - Journal of The Institution of Engineers (India): Series C, 2024<br><br>**Abstract:** Metallic foams offer unique benefits in fields such as energy-absorbing technologies, lightweight structural sandwich panels, and heat sinks due to their exceptional combination of |

| | |
|---|---|
| | properties. These foams exhibit distinct mechanical and physical properties including high porosity, stiffness, lightweight, enhanced damping capacity, and low thermal conductivity. This review focuses on the production methods of metallic foams, categorizing the various manufacturing procedures based on the state of matter—solid, liquid, gaseous, or ionized—in which the metal is processed. Additionally, this paper discusses the behavior of metal foam manufactured by different methods at varying strain rates, using universal testing machines and the split Hopkinson pressure bar for quasi-static and high strain rate testing. |
| **71.** | Pyrene functionalized organic cation receptor-based "turn-on" fluorescence approach for monitoring of chlorpyrifos in food, soil, and water samples<br>**M Kumar, A Dhiman**, G Singh, N Kaur, **N Singh** - Analytica Chimica Acta, 2025<br><br>**Abstract:** Background: The unregulated use of pesticides by farmers, for crop productivity results in widespread contamination of organophosphates in real environmental samples, which is a growing societal concern about their potential health effects. The conventional approaches for the monitoring these organophosphate-based pesticides which include immunoassays, electrochemical methods, immunosensors, various chromatography techniques, along with some spectroscopic methods, are either costly, sophisticated, or involves the use of different metal complexes. Therefore, there is an urgent need for sensitive, quick, and easy-to-use detection techniques for the screening of widely used organophosphate-based pesticides. Results: Herein, we demonstrates the metal-free detection of CPF pesticide in aqueous medium, based on the organic nanoparticles of benzimidazole-based cationic receptor (R1-ONPs), and thoroughly analyzed using advanced techniques such as AFM, FESEM, and DLS etc. The photophysical investigations revealed that developed R1-ONPs exhibited high selectivity towards chlorpyrifos with an enhancement in fluorescence emission. Further, the observed pyrene excimer-based "turn-on" fluorescence mechanism, and the interaction between developed sensor and chlorpyrifos has been validated utilizing $^{1}H$, and $^{31}P$ NMR spectroscopy. The developed sensor can effectively quantify chlorpyrifos up to a detection limit of 18.9 nM ($3\sigma$ method) with a range of 0–120 μM as well as below the cutoff limit set by FAO. Moreover, the real-time application of developed sensor (R1-ONPs) was evaluated to monitor chlorpyrifos in spiked food, water, and soil samples with good (%) recovery. Significance: The development of metal-free, pyrene-excimer-based "Turn-On" fluorescent sensor offers a novel, eco-friendly strategy for the detection of chlorpyrifos in aqueous medium. Additionally, its ability to quantify the chlorpyrifos at levels as low as those set by FAO makes it more efficient tool for monitoring the environmental toxicity ensuring better protection for human, and animal health.<br>  |
| **72.** | Quantum synchronization between two spin chains using pseudo-bosonic equivalence<br>**J Ghildiyal, S Dasgupta, A Biswas** - Physics Letters A, 2025<br><br>**Abstract:** Quantum synchronization among many spins is an intriguing domain of research. In this paper, we explore the quantum synchronization of two finite chains of spin-1/2 particles, via a nonlinear interaction mediated by a central intermediary spin chain. We introduce a novel approach using the Holstein-Primakoff transformation to treat the spin chains as pseudo-bosonic systems and thereby applying the synchronization criteria for harmonic oscillators. Our theoretical framework and numerical simulations reveal that under optimal conditions, the spin chains can achieve both classical and perfect quantum synchronization. We show that quantum synchronization is robust against variations in the number of spins and inter-spin coupling, |

| | |
|---|---|
| | though may be affected by thermal noise. This work advances the understanding of synchronization in multi-spin systems and introduces a generalized synchronization measure for both bosons and fermions. |
| **73.** | Soft computing techniques in multi-criteria recommender systems: A comprehensive review<br>K Anwar, M Wasid, A Zafar, **MA Ganaie**, A Iqbal - Applied Soft Computing, 2024<br><br>**Abstract:** Recommender systems (RS) play a crucial role in aiding decision-making by filtering information and reducing information overload. Multiple approaches such as collaborative filtering, content-based filtering, and hybrid filtering have revolutionized RS. The RS applications is predominantly used in diverse domains such as e-commerce, e-learning, and tourism. The emergence of multi-criteria recommender systems (MCRS) has further enhanced user experiences and satisfaction by incorporating user ratings on various item factors. However, the integration of multi-criteria ratings into RS poses challenges related to multidimensionality, data sparsity, and criteria weight elicitation. To provide accurate recommendations, researchers have proposed a range of soft computing-based MCRS approaches. In this paper, we review and classify the diverse soft computing techniques employed in MCRS. Moreover, we present a compact framework that utilizes soft computing techniques in multi-criteria collaborative filtering-based RS. We anticipate that this paper will benefit researchers engaged in RS and soft computing fields, offering valuable insights for future research and development. |
| **74.** | Stability analysis of time dependent solutions for the coagulation equation with source and efflux<br>D Ghosh, **J Kumar**, A Petrugel - Journal of Nonlinear and Convex Analysis, 2024<br><br>**Abstract:** This article provides mathematical proof of the existence of stationary solutions for the coagulation equation including source and efflux terms. We demonstrate the convergence of time dependent solutions to these stationary solutions and highlight the exponential rate of convergence. These properties are analyzed for affine linear coagulation kernels, non-negative source terms and positive efflux rates. |
| **75.** | Superalkali OLi3 anchored biphenylene for hydrogen storage: Acumen from first-principles study<br>**P Beniwal, TJ Dhilip Kumar** - Journal of Energy Storage, 2025<br><br>**Abstract:** Developing efficient hydrogen storage materials is critical for reducing reliance on conventional fossil fuels in the transportation sector. In this context, we employed first-principles calculations to explore the hydrogen storage potential of biphenylene (BPN) sheets with superalkali $OLi_3$ clusters. With both side coverage, the anchoring of $OLi_3$ clusters to the BPN sheet occurs via a charge transfer mechanism, resulting in strong binding with a calculated binding energy of −3.05 eV per $OLi_3$ cluster. The $OLi_3$ anchored clusters significantly enhances the potential by generating additional active sites, thereby improving $H_2$ adsorption through a combined electrostatic and van der Waals interaction mechanism. In the $2OLi_3$/BPN complex, up to 18 $H_2$ molecules can be effectively adsorbed, with adsorption energies ranging from −0.217 to −0.282 eV, yielding a remarkable gravimetric hydrogen density of 9.11 wt%. This value surpasses the U.S. Department of Energy's benchmark for hydrogen storage, set at 5.5 wt%. Using the van't Hoff equation, the desorption temperature of the $2OLi_3$/BPN+$18H_2$ complex is calculated to be 258 K at 1 atm and 337 K at 5 atm, indicating favorable hydrogen release characteristics. Furthermore, ab initio molecular dynamics simulations confirm both the structural stability of the material and the reversibility of $H_2$ adsorption. With the appropriate $H_2$ adsorption energy, high gravimetric density, and structural stability, it is expected that the use of $OLi_3$ anchored BPN sheets will serve as an effective method with high-capacity reversible hydrogen storage. |

| | |
|---|---|
| | 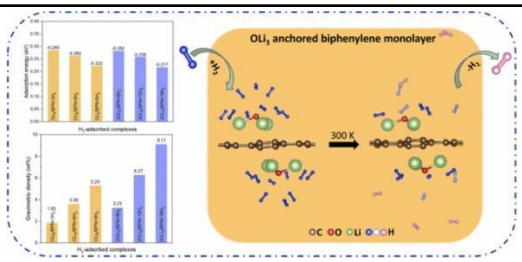 |
| **76.** | Systematic estimation of ηpl factor using load separation analysis in discrete intervals<br>**R Upadhyaya, A Tiwari** - Theoretical and Applied Fracture Mechanics, 2024<br><br>**Abstract:** Standard fracture toughness methods require significant constraint on the specimen, restricting the crack depth, a/W, to 0.45 - 0.70. However, there are situations where shallow cracks need to be analyzed, which requires a suitable correlation factor, $\eta_{pl}$, for determining the J-R curve. The experimentally obtained $\eta_{pl}$ factor is dependent on the level of constraint, and it is expected that a plane stress condition will yield a different $\eta_{pl}$ value for the same material. One conventional method that can be used, both experimentally and numerically, to determine $\eta_{pl}$ factors for unconventional testing specimens and for less constrained cracks, is the load separation method. This work applies and explores the method by which the load separation technique can be accurately employed to determine the $\eta_{pl}$ factor for specimens with shallower cracks. A systematic approach for applying the load separation method for $\eta_{pl}$ factor determination is provided, and it is demonstrated that, under the constraints specified by ASTM E1820, the $\eta_{pl}$ factor aligns with the values presented in the standard. |
| **77.** | The negative modulation index: A key for augmenting solutions in selective harmonic elimination and mitigation strategies<br>**P Kalkal, AVR Teja** - IEEE Transactions on Industrial Electronics, 2024<br><br>**Abstract:** This article explores the innovative application of the negative modulation index (NMI) as a means to broaden the range of viable options for selective harmonic elimination (SHE) and selective harmonic mitigation (SHM) strategies. Conventionally, the use of a positive modulation index has been standard practice to attain the required magnitudes and phases of fundamental components. However, the research discloses that integrating NMI, which induces phase inversion while preserving magnitude, unlocks additional solutions, particularly in areas previously considered intractable. A critical reassessment of the phase-reversal region is conducted, uncovering its untapped potential for unique solutions. Despite the phase inversion introduced by NMI, the article proposes a novel implementation strategy that retains the original phase. The validity of this approach is established through graphical analysis, simulations in MATLAB/Simulink, and practical implementation on an FPGA-based experimental prototype for two, five, and seven switching angles per quarter. A range of case studies are presented that demonstrate significant enhancements in the SHE and SHM techniques through the utilization of NMI, thereby marking a new phase in the progression of harmonic control methods. |
| **78.** | Unleashing high yield urea production by pulse electrodeposition of Bi/Cu *via* co-reduction of $N_2$ and $CO_2$<br>**S Kaur, K Garg, D Gupta, A Kafle, Dharmender, V Shukla, R Ahuja, TC Nagaiah** - ACS Energy Letters, 2024<br><br>**Abstract:** The expanding agricultural practices rely on carbon- and energy-intensive Bosch–Meiser processes for urea synthesis. Alternatively, electrochemical coupling of $CO_2$ and $N_2$ is emerging as a sustainable approach. Unfortunately, the high energy barrier for $N_2$ and $CO_2$ cracking for C–N bond coupling limits the urea synthesis efficiency. Herein, we have electrodeposited Bi on Cu foil *via* triple pulse voltage, and the fabricated Bi(0.01 V)@Cu electrode demonstrates a high yield rate of 646 μg $h^{-1}$ $mg^{-1}_{cat}$ of urea with 70.7% Faradaic |

| | |
|---|---|
| | efficiency at −0.45 V *vs* RHE. The isotopic labeling experiments assert that the produced urea is solely from the dissolved $CO_2$ and $N_2$ gases. More importantly, we have utilized *in situ* electrochemical Raman spectroscopy and Fourier transform infrared (FTIR) measurements to monitor the real-time formation of urea, further supported by a microelectrochemical approach using a Pt-microelectrode and the results were verified by density functional theory (DFT) analysis. Moving a step forward, plant growth and flowering upon addition of extracted urea have been demonstrated for practical application.<br> 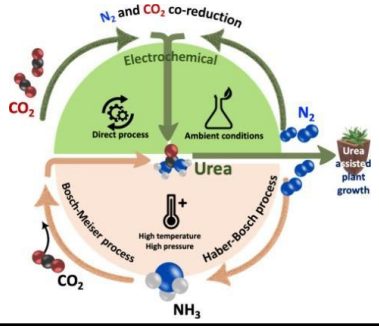 |
| **79.** | Using urban topology to identify critical links of the road network: A centrality-based approach<br>**A Bhamidipati, TM Rahul** - Urban Mobility India, 2024<br><br>**Abstract:** Understanding the urban network's structure is essential to comprehend how a city's traffic moves. A well-planned city can be distinguished from a demand-oriented development, where the road network is created based on traffic demand rather than a plan, using the topology of the road network. Though the usual measures of understanding the formation of a road network, including the road network density, the junction density, average path length, etc., aid in characterizing the road network, they are weak in explaining the importance or influence of specific nodes/links in the network. Betweenness centrality is particularly relevant for understanding urban movement patterns because it quantifies the extent to which a node lies on the shortest paths between other nodes. Nodes with high betweenness centrality are often located on important routes that facilitate efficient transportation and experience a higher flow of traffic. As betweenness centrality highlights the important edges present in a network there should, hypothetically, exist a correlation between the width of the road segments and their corresponding betweenness. The current study aims to mathematically quantify the correlation between the widths of different road segments in the network and their corresponding betweenness centralities. The topological analysis is conducted for the road network of Ludhiana City of Punjab. The final value of correlation is interpreted and further policy implications are discussed. |
| **80.** | Utilizing ground granulated blast furnace slag during carbon sequestration in concrete<br>**SK Saikia, AS Rajput, K Saini** - Journal of Materials in Civil Engineering, 2025<br><br>**Abstract:** Carbon-sequestered concrete (CSC) and green binders such as ground granulated blast furnace slag (GGBFS) have emerged as promising solutions for reducing the environmental impact of concrete. With the aim of optimizing its carbon capture capacity, the authors attempted to evaluate and enhance the carbon sequestration of GGBFS-added concrete types using cutting-edge $CO_2$ mixing and $CO_2$ curing facilities. Micromechanical tests were performed to determine the impact of $CO_2$ sequestration on the microstructure, strength, and porosity of concrete prepared using this novel binder, which replaced 50% of the conventional cement. Its use demonstrated an encouraging $CO_2$ uptake of up to 20% and improved compressive strength on account of thermodynamically stable calcite polymorph formation, resulting in microstructural densification. Additionally, it could be observed that the $CO_2$ mixing process was uniform, with a conversion rate of 63.41%, whereas $CO_2$ curing was a surface-controlling phenomenon with 96.18% conversion. |

**Disclaimer:** This publication digest may not contain all the papers published. Library has compiled the publication data as per the alerts received from Scopus and Google Scholar for the affiliation “Indian Institute of Technology Ropar” for the month of December, 2024. The author(s) are requested to share their missing paper(s) details if any, for the inclusion in the next publication digest.